



**British  
Geological Survey**

NATURAL ENVIRONMENT RESEARCH COUNCIL

# CLiDE Version 1.0 User Guide

Environmental Modelling Programme

Open Report OR/14/011

BRITISH GEOLOGICAL SURVEY

ENVIRONMENTAL MODELLING PROGRAMME

OPEN REPORT OR/14/011

# CLiDE Version 1.0 User Guide

A.Barkwith\* and T.J. Coulthard\*\*

The National Grid and other Ordnance Survey data are used with the permission of the Controller of Her Majesty's Stationery Office. Ordnance Survey licence number Licence No:100017897/2013.

## Keywords

Climate change; Soil Moisture; Electrical Earthing; Hydrology; UKCP09 scenarios.

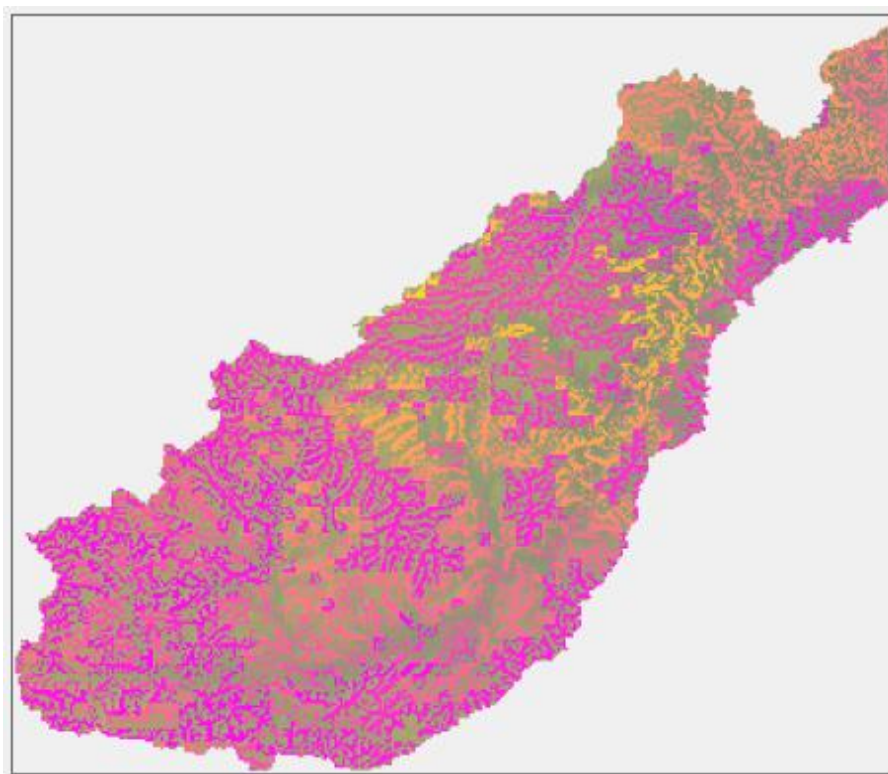
## Bibliographical reference

Barkwith, A. and Coulthard, T.J.. 2013. CLiDE Version 1.0 User Guide. British Geological Survey Open Report, OR/14/011. 54pp.

Copyright in materials derived from the British Geological Survey's work is owned by the Natural Environment Research Council (NERC) and/or the authority that commissioned the work. You may not copy or adapt this publication without first obtaining permission.

Contact the BGS Intellectual Property Rights Section, British Geological Survey, Keyworth, e-mail [ipr@bgs.ac.uk](mailto:ipr@bgs.ac.uk) You may quote extracts of a reasonable length without prior permission, provided a full acknowledgement is given of the source of the extract.

© NERC 2013. All rights reserved



\* *British Geological Survey, Environmental Science Centre, Keyworth, Nottingham, NG12 5GG, UK*

\*\* *Department of Geography, Environment and Earth Science, University of Hull, Cottingham Road, Hull, HU6 7RX, UK*

Keyworth, Nottingham British Geological Survey 2013

## BRITISH GEOLOGICAL SURVEY

The full range of Survey publications is available from the BGS Sales Desks at Nottingham, Edinburgh and London; see contact details below or shop online at [www.geologyshop.com](http://www.geologyshop.com)

The London Information Office also maintains a reference collection of BGS publications including maps for consultation.

The Survey publishes an annual catalogue of its maps and other publications; this catalogue is available from any of the BGS Sales Desks.

*The British Geological Survey carries out the geological survey of Great Britain and Northern Ireland (the latter as an agency service for the government of Northern Ireland), and of the surrounding continental shelf, as well as its basic research projects. It also undertakes programmes of British technical aid in geology in developing countries as arranged by the Department for International Development and other agencies.*

*The British Geological Survey is a component body of the Natural Environment Research Council.*

*British Geological Survey offices*

### **Keyworth, Nottingham NG12 5GG**

☎ 0115-936 3241 Fax 0115-936 3488  
e-mail: [sales@bgs.ac.uk](mailto:sales@bgs.ac.uk)  
[www.bgs.ac.uk](http://www.bgs.ac.uk)  
Shop online at: [www.geologyshop.com](http://www.geologyshop.com)

### **Murchison House, West Mains Road, Edinburgh EH9 3LA**

☎ 0131-667 1000 Fax 0131-668 2683  
e-mail: [scotsales@bgs.ac.uk](mailto:scotsales@bgs.ac.uk)

### **London Information Office at the Natural History Museum (Earth Galleries), Exhibition Road, South Kensington, London SW7 2DE**

☎ 020-7589 4090 Fax 020-7584 8270  
☎ 020-7942 5344/45 email: [bgs london@bgs.ac.uk](mailto:bgs london@bgs.ac.uk)

### **Forde House, Park Five Business Centre, Harrier Way, Sowton, Exeter, Devon EX2 7HU**

☎ 01392-445271 Fax 01392-445371

### **Geological Survey of Northern Ireland, Colby House, Stranmillis Court, Belfast BT9 5BF**

☎ 028-9038 8462 Fax 028-9066 2835  
e-mail: [gsni@detini.gov.uk](mailto:gsni@detini.gov.uk)

### **Maclean Building, Crowmarsh Gifford, Wallingford, Oxfordshire OX10 8BB**

☎ 01491-838800 Fax 01491-692345  
e-mail: [hydro@bgs.ac.uk](mailto:hydro@bgs.ac.uk)

### **Sophia House, 28 Cathedral Road, Cardiff, CF11 9LJ**

☎ 029-2066 0147 Fax 029-2066 0159

*Parent Body*

### **Natural Environment Research Council, Polaris House, North Star Avenue, Swindon, Wiltshire SN2 1EU**

☎ 01793-411500 Fax 01793-411501  
[www.nerc.ac.uk](http://www.nerc.ac.uk)

# Contents

<b>Contents</b>	<b>i</b>
<b>1 Introduction</b>	<b>1</b>
1.1 Background	1
1.2 User Guide	1
<b>2 Component Summary</b>	<b>2</b>
2.1 Introduction	2
2.2 Water Partitioning Component	3
2.3 Surface Water Routing Component	4
2.4 Groundwater Component	4
2.5 Sediment Transport Component	6
2.6 Vegetation Component	9
2.7 Debris Flow Component	9
2.8 Climate Change Component	12
<b>3 CLiDE Pre-processing</b>	<b>13</b>
3.1 Introduction	13
3.2 Software	13
3.3 Input File Properties	13
3.4 Graphical User Interface	15
3.5 Discretisation	17
3.6 Meteorology	20
3.7 Surface Partitioning	22
3.8 Groundwater	26
3.9 Lisflood Surface Flow	28
3.10 Sediment	29
3.11 Vegetation	32
3.12 Slope Processes	32
3.13 Climate Factors	35
<b>4 CLiDE Model</b>	<b>36</b>
4.1 Introduction	36
4.2 Initialisation	36
4.3 Runtime	37
4.4 Save Options	38
4.5 Graphical Options	39
<b>5 Calibration</b>	<b>40</b>
5.1 Introduction	40
5.2 Hydrological	40

5.3 Debris Flow	42
<b>6 Troubleshooting</b>	<b>43</b>
<b>References</b>	<b>45</b>

## FIGURES

Figure 1 - Schematic overview of the main linkages between the CLiDE platform hydrological components. Dashed lines represent data required from the previous timestep and solid lines data from the current timestep. ....	2
Figure 2 - Variation in the failure angle for a shallow landslide as a function of soil moisture and the internal friction angle follow infinite slope stability analysis (see equation 2.23). Cohesion was assumed negligible ( $C^*$ set to zero). Increased soil moisture causes a reduction in the angle up to which hillslopes might be stable.....	12
Figure 3 - The CLiDE GUI under the <i>setup</i> tab.....	15
Figure 4 - The GUI after the simulation input data has been loaded into the model .....	17
Figure 5 - First six lines of a rainfall file, specifying the spatial attributes of the data. The next two lines show the beginning of the dataset ( $\text{mm d}^{-1}$ ).....	20
Figure 6 - An example of a PE List file. The first line is a header, and the remaining lines comma-separated, time-stamped, potential evapotranspiration ( $\text{kg m}^{-2}\text{s}^{-1}$ ) data for each identifier over the length of the simulation. ....	21
Figure 7 - The PE Numbers file contains a list of the identifiers used in the PE gridded file. The first line is a header and the second a white-space separated list of identifiers.....	21
Figure 8 - Hydrological tab parameters in the GUI .....	23
Figure 9 - Example surface water discharge file. The first line defines the coordinates of the outflow nodes and the following line the daily water outflow ( $\text{m}^3$ ) from that node. ....	26
Figure 10 - Flow model (Lisflood) tab parameters in the GUI .....	28
Figure 11 - Sediment tab parameters in the GUI .....	30
Figure 12 - Slope Process tab parameters in the GUI .....	33
Figure 13 - Snapshot of the CLiDE GUI displaying changes to groundwater levels after 348 days of simulation .....	37

**TABLES**

Table 1 - Input files for the CLiDE platform ..... 14

Table 2 - The upper tabs available in the GUI and description of their parameters ..... 16

Table 3 - Hydrological boundary conditions for the CLiDE platform. \*Numbers have been reserved for this boundary type but it has not yet been implemented in the model code. .... 22

Table 4 – Landuse habitat numbers and associated descriptions (Morton et al., 2011)..... 24

Table 5 – Definition of the 29 HOST soil class numbers (modified from Boorman et al., 1995). The remaining two classes (30 and 31) are used to describe surface water features. The integrated air capacity (IAC - is the average percentage air volume over a depth of one metre) is used to differentiate some classes. .... 25

# 1 Introduction

## 1.1 BACKGROUND

The Dynamic Environmental Sensitivity to Change (DESC) project coupled cellular automaton (CA) modelling from various backgrounds and produced the CAESAR-Lisflood-DESC (CLiDE) modelling platform: a geomorphological simulator that allows a variety of Earth system interactions to be explored. A derived version of the well established Cellular Automaton Evolutionary Slope and River (CAESAR) model (Coulthard and Van De Wiel, 2006), CAESAR-Lisflood, which incorporates the Lisflood hydrodynamic model (Coulthard et al., 2013) to simulate channel and overbank flow, is used as the platform kernel. The two dimensional modular design allows great versatility in the range of simulated spatio-temporal scales to which it can be applied. CAESAR has been used to investigate a variety of sediment transport, erosional and depositional processes under differing climatic and land use pressures in river reaches and catchments (Hancock et al., 2011). The recent addition of Lisflood to the code improves the representation of surface water flow within the model by incorporating momentum. However, as with many landscape evolution models (LEMs), CAESAR over-simplifies the representation of some of the hydrological processes and interactions that drive sediment transport. Specifically, it does not simulate groundwater flow and its discharge to rivers. To address these limitations, the non-Lisflood controlled surface hydrological processes within the CLiDE platform are replaced with a bespoke distributed hydrological model that includes a groundwater model. This hydrological model partitions rainfall between surface run-off and recharge to groundwater using a soil water balance model, which is applied at each grid cell. To simulate groundwater flow to river channels we incorporate a single layer finite difference model into the code. This solves the governing partial differential groundwater flow equation using a forward time-stepping, or explicit, solution method (Wang and Anderson, 1982), which can be considered as a cellular automaton (CA) model (Ravazzani et al., 2011). The groundwater model is coupled to the surface model through the exchange of recharge and baseflow. In addition to the hydrological modifications, a debris flow component has been added to the platform. The triggering aspect of this component is linked to simulated groundwater levels.

## 1.2 USER GUIDE

This manual is designed to guide a new user through the process of setting up the CLiDE platform for a desired catchment, calibrating the model and undertaking a simulation. Also included is an explanation of the governing components of the CLiDE platform, the required input files and a troubleshooting section. Post-processing is not explicitly discussed, as this process is individual to each project, however a description of the output files is provided to aid this process.



## 2 Component Summary

### 2.1 INTRODUCTION

This section introduces the major components of the CLiDE platform and their driving equations. Many of the components interact with each other, providing information about differing parameters at a range of time steps. The hydrological component (SLiM) employs a surface water partitioning module to divide water between the atmosphere, the surface and subsurface (Figure 1). The groundwater module dictates the flow of subsurface water and Lisflood the flow of surface water. These two components interact directly through the passing of baseflow to rivers and indirectly through the calculation of groundwater recharge by SLiM. Sediment transport is divided into fluvial and non-fluvial processes. The fluvial sediment transport processes are dictated by the hydrological component, in particular Lisflood, which provide the energy to move sediment of differing grain sizes. Non-fluvial sediment transport processes can also be affected by hydrology, for example high groundwater water levels can trigger debris flows within the SCIDDICA debris flow module.

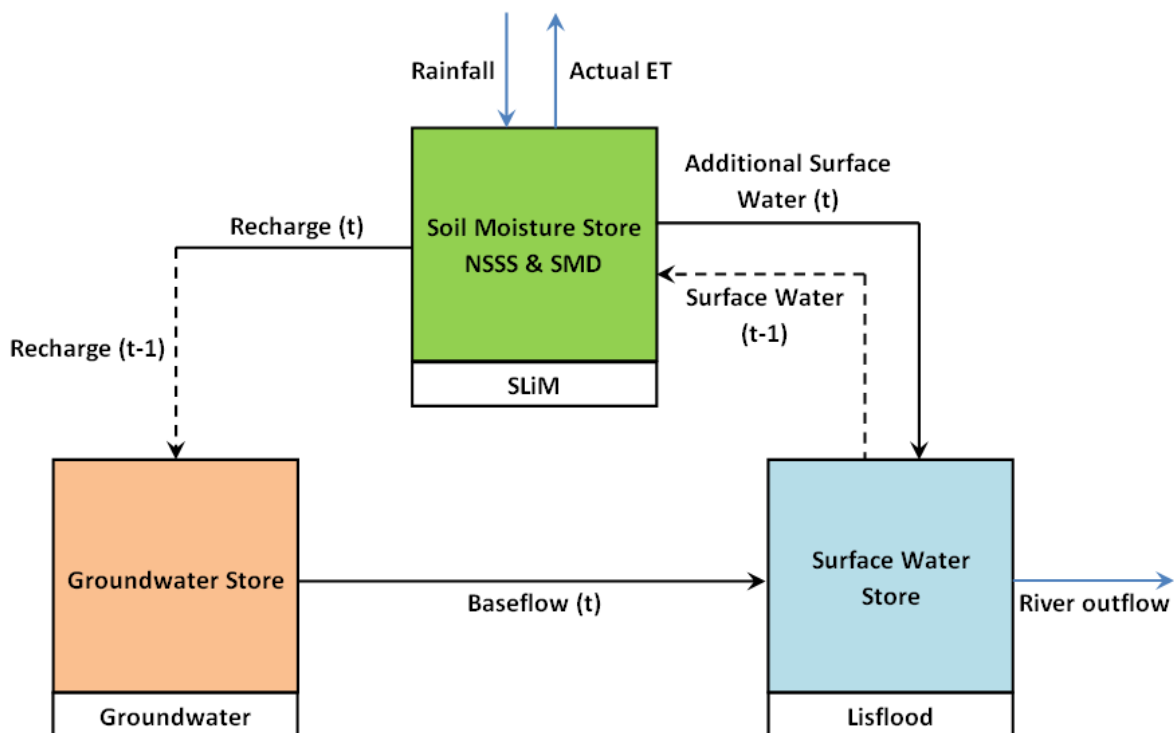


Figure 1 - Schematic overview of the main linkages between the CLiDE platform hydrological components. Dashed lines represent data required from the previous timestep and solid lines data from the current timestep.

## 2.2 WATER PARTITIONING COMPONENT

The partitioning of rainfall between, evaporation, runoff and recharge to groundwater in the CLiDE platform is achieved using the soil water partitioning model SLiM (Wang et al., 2012). SLiM implements a simple technique that represents potential groundwater recharge and runoff processes based on spatio-temporally distributed soil moisture conditions. Soil moisture is a function of; rainfall, actual evapotranspiration, soil moisture condition, topography, soil type, crop type and baseflow properties. This method represents soil water processes responding to variable soil water storage properties (see Rushton, 2003) and vegetation growth stages (see Allen et al., 1998).

Within SLiM, rainfall that isn't evaporated, or doesn't contribute directly to runoff, can be either intercepted by plants or reach the ground surface and infiltrate into the soil. The latter has the effect of increasing near surface soil storage and reducing the soil moisture deficit (*SMD*). Soil water can be extracted by plant roots for transpiration or drawn to the bare soil surface for evaporation. When soil moisture reaches field capacity and is unable to store further additions of water, water drains freely in the saturated soil. At field capacity if there are additional water inputs, lateral runoff (routed by Lisflood) occurs if a gradient exists towards adjacent locations. If the rainfall intensity is greater than the capacity of soil to maintain infiltration, water accumulates on the soil surface and becomes surface runoff. Water not accounted for in soil storage, evapotranspiration or uptake by vegetation is termed *excess water* ( $E_w$ ). Excess water is divided between runoff ( $R_o$ ) and recharge to groundwater ( $R_e$ ) based on a baseflow index parameter (*BFI*). The *BFI* may be derived through a calibration process or estimated from data by performing a baseflow separation on a river flow time-series. Surface runoff and recharge to groundwater are calculated using equations 2.1 and 2.2:

$$R_e = E_w \cdot BFI \quad (2.1)$$

$$R_o = E_w (1 - BFI) \quad (2.2)$$

*BFI* is an average surface to subsurface water partitioning ratio reflecting the permeable nature of the catchment in addition to other catchment characteristics. In general greater runoff and reduced recharge is observed in areas with steeper slopes. Consequently equations 2.1 and 2.2 are modified to allow average ( $\bar{S}$ ) and nodal ( $S$ ) terrain gradient to be factored into the calculation of recharge and runoff:

$$R_o = \frac{E_w \cdot (1 - BFI) \cdot S}{\bar{S}} \quad (\text{if } S \leq \bar{S}) \quad (2.3)$$

$$R_o = \frac{(S - \bar{S}) \cdot E_w \cdot BFI}{(90 - \bar{S})} + \bar{S} \quad (\text{if } Slp > \bar{S}) \quad (2.4)$$

$$R_e = E_w - R_o \quad (2.5)$$

### 2.3 SURFACE WATER ROUTING COMPONENT

Routing of surface runoff and channel flow is controlled by Lisflood (Van der Knijff et al., 2010), a two-dimensional hydrodynamic flow model. Routing is based on the one dimensional Saint-Venant equations, as modified by Bates et al. (2010), where the derived equation (2.6) takes into account; acceleration, water surface gradient and friction properties and has enhanced stability due to increased friction forcing water flow towards zero (Liang et al., 2006):

$$q_{t+dt} = \frac{q_t - gh_f dt S}{1 + gh_f dt n^2 q_t / h_f^{3.33}} \quad (2.6)$$

If the flow depth ( $h_f$ ), as calculated using the surface partitioning component, is above a defined threshold and stability criteria are met, the flux between cells at the proceeding time-step ( $q_{t+dt}$ ) depends on the water surface gradient between the adjacent cells ( $S$ ), Manning's coefficient ( $n$ ), the time-step length ( $dt$ ) and the gravitational constant ( $g$ ). For each time-step flow between neighbouring cells is computed and flow depths updated simultaneously at all points within the model domain. A full description of CAESAR-Lisflood is provided by Coulthard et al. (2013).

### 2.4 GROUNDWATER COMPONENT

Groundwater flow is simulated using a two dimensional lattice of square cells interacting according to the von Neumann type neighbourhood, in a technique similar to that utilised by Rothman (1988). Cells consist of distributed hydraulic conductivity ( $k$ ) and specific yield ( $Sy$ ), and a datum referenced aquifer head ( $h$ ) that is modified through time. Aquifer head is updated at each time-step using Darcy's law to calculate water flux ( $q_{gw}$ ) between cells  $i$  and  $j$ :

$$q_{gw} = \frac{2T_i T_j}{T_i + T_j} (h_i - h_j), \quad (2.7)$$

where transmissivity ( $T$ ) can be approximated by multiplying hydraulic conductivity by aquifer depth. The term  $2T_i T_j / (T_i + T_j)$  is introduced as a flux limiter to improve stability when large outliers in transmissivity are encountered. The total flux for a central cell ( $q_{gwt}$ ) is a combination of; fluxes to neighbouring cells and additional source and sink terms. Recharge from the surface hydrological component provides the source term and baseflow to the surface acts as a sink. Total fluxes are used to update aquifer heads at each point in the domain simultaneously at each time step ( $dt$ ) using the discrete mass balance equation:

$$h_{t+dt} = h_t + \frac{1}{Sy} \frac{q_{gwt}}{ds^2} dt \quad (2.8)$$

Two user defined lateral boundary condition types have been implemented into the CLIDE code, allowing a variety of hydrological situations to be represented. Specified (Dirichlet) boundary conditions fix aquifer head at the boundary to the initial condition and a no-flow (Neumann B) condition sets flux across the boundary to zero. The base of the aquifer is defined as impermeable; however, leakage from the base of the modelled aquifer is included in the flux algorithm as a secondary sink term. The surface boundary allows a flux of water to be returned to the surface component as baseflow where aquifer head is greater than terrain height.

To ensure model stability, the cell Reynolds number ( $Rn$ ) is calculated at each node for each time-step and a flag raised if it exceeds unity. Reduction of the Reynolds number is possible by reducing the time-step or increasing the cell size. Roache (1976) defines the Reynolds number as:

$$Rn = 4 \frac{T}{Sy} \frac{dt}{dx^2} \quad (2.9)$$

Baseflow return to rivers at regions where the groundwater head is at a greater elevation than the surface water ( $r$ ) for a particular node. The volume of water returned to rivers ( $q_{bf}$ ) is dependent on the specific yield of the groundwater node and the thickness ( $RB_b$ ) and hydraulic conductivity ( $RB_k$ ) of the river bed using the equation derived by Haitjema (1995):

$$q_{bf} = Sy \left( \frac{h-r}{c} dx^2 \right) \quad (2.10)$$

$$c = \frac{RB_b}{RB_k} \quad (2.11)$$

## 2.5 SEDIMENT TRANSPORT COMPONENT

There are several sediment transport models that can be used to evaluate landscape evolution at the decadal to centennial timescales required for the CLiDE. Coulthard (2001) reviews these, and an overview of the theory behind modelling landscape evolution is presented by Tucker and Hancock (2010). The ability of current models to employ distributed fluvial and erosional processes gives an advantage over previous approaches (see Kinnell, 2010), as they are based on DEMs, include distributed soil depths, allow surface runoff and can automatically determine inter-cell slope gradient and transport of sediment. For this study CAESAR was selected to provide the sediment transport and Graphical User Interface (GUI) properties for the CLiDE platform as it has a modular, versatile design and has been validated in a range of environmental settings. The reduced complexity cellular automaton (CA) nature of CAESAR facilitates simulation of regional scale catchments, with a high resolution spatio-temporal discretisation, at a relatively low computational cost. A novel cell scanning algorithm removes the need to employ grid sorting techniques, further reducing computation cost, and allows lateral surface flow diversion and conversion to be simulated. Due to its adaptable nature, CAESAR has been used for many applications including: modelling the response of river systems to environment change (Van De Wiel et al., 2011), urban drainage management (Coulthard and Frostick, 2010), human impact on fluvial regimes and fluxes of sediment (Hoffmann et al., 2010), influences of vegetation on river development (Tooth et al., 2008), catchment response to environmental change (Coulthard et al., 2005), and more recently determining catchment soil loss rates (Hancock et al., 2011).

The remainder of this section describes the major features of CAESAR that have been retained by the CLiDE platform. CAESAR incorporates a scanning algorithm based upon the Moore neighbourhood of cells, similar to that used by Murray and Paola (1994, 1997), to monitor the properties of surrounding cells. As with the hydrological model, space is discretised into a two-dimensional lattice of square cells; however, to increase stability and reduce computational cost, time-steps are not uniform and reduce as the anticipated amount of sediment flux increases. Tracking simulated time ( $t$ ) allows inputs from coupled modules and some internal functions to be calculated on a regular time-

step, reducing computational stress. Initial surface elevation is input from a grid referenced DEM that is modified as time progresses.

A modified version of TOPMODEL (Bevan and Kirkby, 1979), a physically based, watershed model that simulates surface fluxes of water was initially used by CAESAR to derive the partitioning and routing of surface water. The algorithms that deal with the surface routing were subsequently replaced with Lisflood, improving the representation of channel flow and flooding events. The remaining TOPMODEL water partitioning algorithms were not desirable for the CLiDE platform. They do not provide the distributed soil moisture or recharge properties required to simulate the variety of environmental systems represented by current or potential future CLiDE modules (for example; landslides, dynamic vegetation, or groundwater). For this reason TOPMODEL was replaced in the platform by the bespoke coupled surface-subsurface hydrological model. The coupled component supplies surface water depths and flow properties needed by the CAESAR component to calculate sediment transport.

After flow depths have been updated, fluvial erosion and deposition are calculated, where fluvial sediment transport is determined using either the Wilcock and Crowe method, to calculate mixed-size particle movement (Wilcock and Crowe, 2003), or the Einstein-Brown method to calculate particle movement of a single grainsize (Einstein, 1950).

The Wilcock and Crowe formulation (equation 2.12) uses the fractional volume of a particular sediment size ( $F_i$ ), shear velocity ( $u_*$ ), ratio of sediment to water density ( $s$ ), gravity ( $g$ ), and the function  $W_i$ (equation 2.13); which allows the total transport to be calculated (equation 2.14) from the fractional grain shear stress ( $\tau$ ) and a reference sheer stress ( $\tau_{ri}$ ):

$$q_{sed} = \frac{F_i u_*^3 W_i}{(s-1)g} \quad (2.12)$$

$$W_i = 0.002(\Phi)^{7.5} \quad \text{for } \Phi < 1.35 \quad (2.13)$$

$$= 14 \left( 1 - \frac{0.894}{\Phi^{0.5}} \right)^{4.5} \quad \text{for } \Phi \geq 1.35$$

$$\Phi = \frac{\tau}{\tau_{ri}} \quad (2.14)$$

The Wilcock and Crowe method can transport sediment within a catchment as both a suspended load and a bedload (Equation 2.15). Both depend on the volume of sediment transported per time-step, where the sediment transported from a central cell to a neighbouring cell ( $k$ ) is calculated by equating the coefficient  $X$  to either; slope, for bedload transport, or velocity for suspended load transport. The calculation of suspended load transport is simplified, as it assumes an equal distribution of sediment throughout the water column. Sediment deposition also differs between the two transport types, with bedload sediment deposited (and subsequently re-entrained) at every time-step and suspended sediment deposition based on fall velocities.

$$V = \frac{X_k}{\sum X} q_{sed} dt \quad (2.15)$$

Under a quasi-uniform sediment grain size regime the less computationally expensive Einstein method for transport may be employed. The formulation uses the relative density of submerged sediment ( $\rho_s - \rho$ ), grain size ( $D$ ), flow depth and the water surface gradient to evaluate the forces ( $\psi$ ) moving and restraining a particle (equation 2.16). A bedload transport rate can be calculated from these forces and used to approximate the flux of sediment ( $q_{sed}$ ) between cells (equation 2.17). The amount of sediment that can be transported is calculated and moved from the erodible layer.

$$\psi = \frac{(\rho_s - \rho) D}{\rho h_f S} \quad (2.16)$$

$$q_{sed} = \frac{40 \left( \frac{1}{\psi} \right)^3}{\left( \frac{\rho}{(\rho_s - \rho) g D^3} \right)^{0.5}} \quad (2.17)$$

Non-fluvial sediment transport occurs through instantaneous debris flow and a slower creep process. Debris flow is computed using either a two-dimensional sand pile algorithm (Metha and Barker, 1994), based on a critical slope angle, or a more complex model based on the SCIDDICA shallow landslide model (D’ambrosio et al., 2003; Di Gregorio et al., 1999). Both techniques use an iterative process, contained within a single time-step, to move material down slope to lower cells until the model is no longer out of equilibrium. Soil creep ( $Cr$ ) is calculated using a gradient in elevation between cells on a monthly basis through the diffusion equation:

$$Cr = \frac{S \left( \frac{0.01}{12} \right)}{dx}, \quad (2.18)$$

where  $S$  is difference in terrain elevation between cells.

## 2.6 VEGETATION COMPONENT

Vegetation cover in the model is implemented by specifying areas where vegetation covers the surface layer, which has the effect of binding sediment and reducing erodability (see Murray and Paola, 2003). A simple alluvial vegetation growth model is included, allowing linear growth of vegetation over time if it is not submerged. When vegetation has grown beyond a specified limit it restricts fluvial erosion to a percentage of that for uncovered sediment (default value is 10%). If flow shear stress exceeds a threshold the vegetation can be removed – thus exposing the sediment below to unhindered erosion. If vegetation becomes covered by sediment it can re-grow through the sediment layer, thus re-stabilising it.

## 2.7 DEBRIS FLOW COMPONENT

Shallow landsliding and debris flows are important mechanisms by which sediment is redistributed and delivered to the stream network. Most LEMs to date have relied on process-based rules to approximate the influence of landslides over long timescales (Dietrich et al., 2003; Korup et al., 2010). The CLiDE platform simulates shallow landslides and resulting debris flows using the SCIDDICA model (D’ambrosio et al., 2003; Di Gregorio et al., 1999). The model incorporates the changes in energy and water content associated with the flow and the resulting redistribution of debris and is triggered by evolving DEM and hydrological conditions.



The condition for debris flow initiation within SCIDDICA is based on infinite slope stability analysis (Selby, 1993) and computes the balance of driving and resisting forces operating on the hillslope. Infinite slope stability is a widely adopted approach for linking landslide hazard prediction to hydrological models. The model assumes that the length of the slope is several times the soil thickness and that lateral forces are negligible, an assumption that is unlikely to hold in topographic hollows where shallow landslides are commonly triggered (Reneau and Dietrich, 1987). The driving (shear) stress ( $S_d$ ) acting to move soil down a slope is given by the thickness of soil ( $h_s$ ), the density of soil ( $\rho_s$ ), and the angle of the slope ( $\theta$ ) they are acting on:

$$S_d = \rho_s g h_s \sin \theta \cos \theta \quad (2.19)$$

where  $g$  is acceleration due to gravity. On a stable hillslope,  $S_d$  is exceeded by frictional resisting strength  $S_r$  (shear strength), which is the product of the stress acting normal to a potential failure plane ( $\sigma n$ ) and a friction coefficient which is the tangent of the internal friction angle  $\phi$ . The internal friction angle combines the plane friction resulting from when two grains are trying to slide past each other, and friction generated by grain interlocking within the mass (Carson and Kirkby, 1972). Shear strength is given by the Coulomb equation:

$$S_r = C + (\rho_s h_s - \rho_w h_w) g \cos^2 \theta \tan \phi, \quad (2.20)$$

where  $C$  is the effective cohesion within the soil,  $\rho_w$  is water density and  $h_w$  is the elevation of groundwater heads above the potential failure plane. Equating the condition for hillslope failure  $S_d > S_r$  and simplifying results in the trigger condition for landslide initiation (e.g. Pack et al., 2001; Rosso et al., 2006):

$$\tan \theta > C^* + \left( 1 - \frac{\rho_w h_w}{\rho_s h_s} \right) \tan \phi, \quad (2.21)$$

where  $C^*$  is a dimensionless cohesion parameter defined as:

$$C^* = \frac{C}{\rho_s g h_s} \quad (2.22)$$

The hydrologic influence on slope stability is accounted for in the second bracketed term in equation 2.21. The pore pressure ( $u$ ) acting on a potential failure plane is a product of  $P_{hw}$  and  $\rho_w$ . By taking the ratio of  $SMD$ , produced by the SLiM water partitioning module (Section 2.2), to the total available pore space ( $m_c$ ), the soil will be dry when ratio is 1:1 or when  $P_{hw}$  divided by  $SO_b$  is zero in equation 2.21. Alternatively the soil will be saturated when;  $SMD$  is zero and  $SMD$  divided by  $mc$  equals zero or when  $P_{hw}$  equals  $SO_b$ . Thus we can replace  $P_{hw} / SO_b$  with  $(m_c - SMD)/mc$  in equation 2.23:

$$\tan \theta > C^* + \left( 1 - \frac{\rho_w}{\rho_s} \frac{m_c - SMD}{m_c} \right) \tan \phi \quad (2.23)$$

The failure angle decreases with increasing moisture content due to loss of shear strength. Potential angle of failure can be lower than 20° for soils with lower internal friction angles which could result in the prediction of widespread slope failure if cohesion is not taken into consideration. Currently the landslide trigger condition within SCIDDICA assumes that the soil is permanently saturated so that for a prescribed internal friction angle, the failure angle would be given by the right hand edge of Figure 2. Equations 2.21 and 2.23 describe the link between stability and the hydrological conditions modelled within the CLiDE platform.

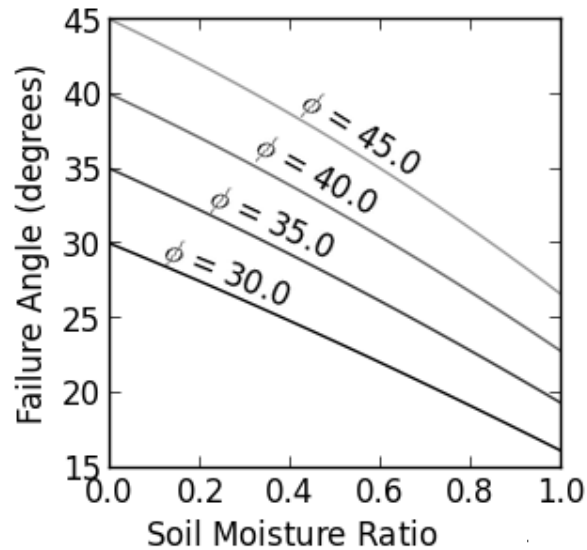


Figure 2 - Variation in the failure angle for a shallow landslide as a function of soil moisture and the internal friction angle follow infinite slope stability analysis (see equation 2.23). Cohesion was assumed negligible ( $C^*$  set to zero). Increased soil moisture causes a reduction in the angle up to which hillslopes might be stable.

## 2.8 CLIMATE CHANGE COMPONENT

Future changes in climate are likely to modify local and global temperatures and change rainfall patterns. This will lead to a modification in the distribution of river flow, soil water content and groundwater levels. Prediction of changes to future distributed precipitation and potential evapotranspiration is common place in global circulation models (GCMs) and downscaled regional climate models (RCMs), such as those encompassed by the UKCP09 dataset. Using these datasets we can simulate the effect of predicted future climate on surface hydrology, groundwater and the partitioning of water amongst the various stores.

The water partitioning model in the CLiDE platform uses a time series of distributed precipitation and potential evapotranspiration to drive surface and subsurface flow. The influence of climate change may be introduced by perturbing the input rainfall and potential evapotranspiration data on a monthly basis (see Section 3.13).

## 3 CLiDE Pre-processing

### 3.1 INTRODUCTION

This section introduces the setup, simulation process and required input data for the CLiDE platform. A brief description on how to access the platform source code is described in Section 3.2, followed by an overview of the different input file structures in Section 3.3. The graphical user interface (GUI) (Section 3.4) allows users to select input data, load initialisation files and view run-time imulation information. Finally model spatial and temporal discretisation is discussed (Section 3.5) and a description of each input parameter presented (Section 3.6 to Section 3.13).

### 3.2 SOFTWARE

Running The CLiDE platform software is straightforward on the windows platform. The model-component portion of the package is self contained in an exe file. The CLiDE source code for the c# visual studio compiler (10 or higher) is contained with the executable in a zip file, accessible using freely available software. The CLiDE platform may be built to run on a single-processor machine or a shared-memory machine through utilisation of the OpenMP API.

The CLiDE platform code has a fairly simple build mechanism. It tries to determine the windows architecture that you are running (32 or 64 bit), and then presents you with options to allow you to select the preferred build method. A description of the build process and components is contained below:

- Obtain the CLiDE zipped file from <http://www.bgs.ac.uk>
- Always get the latest version if you are not trying to continue a long project, or duplicate previous work
- Unzip the file and extract contents
- Open the *CLiDE.csproj* file in visual studio
- In the solution explorer panel, right click *CLiDE.cs* to view the main source code

The code can be compiled in the standard way, either as a debug or release executable. Control of the build, parallel, icon and reference properties can be assessed from the solution explorer panel.

### 3.3 INPUT FILE PROPERTIES

The philosophy behind the structure of the CLiDE platform input, is to separate different types of data between files. That is, each file contains one specific type of information only. Whilst this results in

the model requiring many input files compared to other models, they all have a very simple format and are easily modified using a text editor. For example, one file contains all information relating to hydraulic conductivity, another to soil depth, and another to surface water depth. Examples of all these files are contained in the supplied zip file that contained the executable. These are in the correct format but the data contained within requires tailoring to the user specification.

The list of input files required by CLiDE is presented in Table 1. Though there are thirteen files listed, not all of these are required for a simulation. For example, if grain sizes are set in the user interface, the grain size input file is not needed. The files can be renamed as the user desires as long as the relevant information is updated in the user interface.

Table 1 - Input files for the CLiDE platform

<b>Input File</b>	<b>Relevant Section</b>
Bedrock	3.5.2
DEM	3.5.1
Distributed Hydraulic Conductivity	3.8.2
Distributed Specific Yield	3.8.3
Grain Size	3.5.3
HOST	3.7.4
Initial Debris Thickness	3.12.3
Initial Soil Moisture Deficit	3.7.1
Landuse	3.7.3
PE Grid	3.6.2
PE List	3.6.2
NSSS	3.7.2
Precipitation	3.6.1
Initial Surface Water	3.7.5
Surface Water Influx	3.7.6
Initial Groundwater Heads	3.8.1
Hydrological Boundary	3.6.3
PE Numbers	3.6.2

### 3.4 GRAPHICAL USER INTERFACE

The Graphical User Interface (GUI) for the CLiDE platform is launched when the executable is opened (Figure 3). The GUI allows users to populate the model, set parameters, decide on model output, launch simulations and visualise model progression during run-time. The GUI is arranged into bars (along the top of the GUI) and upper and lower series of tabs. The bars allow configuration files to be saved and uploaded, runtime graphics to be selected, and model output files at particular intervals to be specified. The tabs provide model input and runtime properties for different components of the model. Table 2 gives a brief description of the upper tabs.

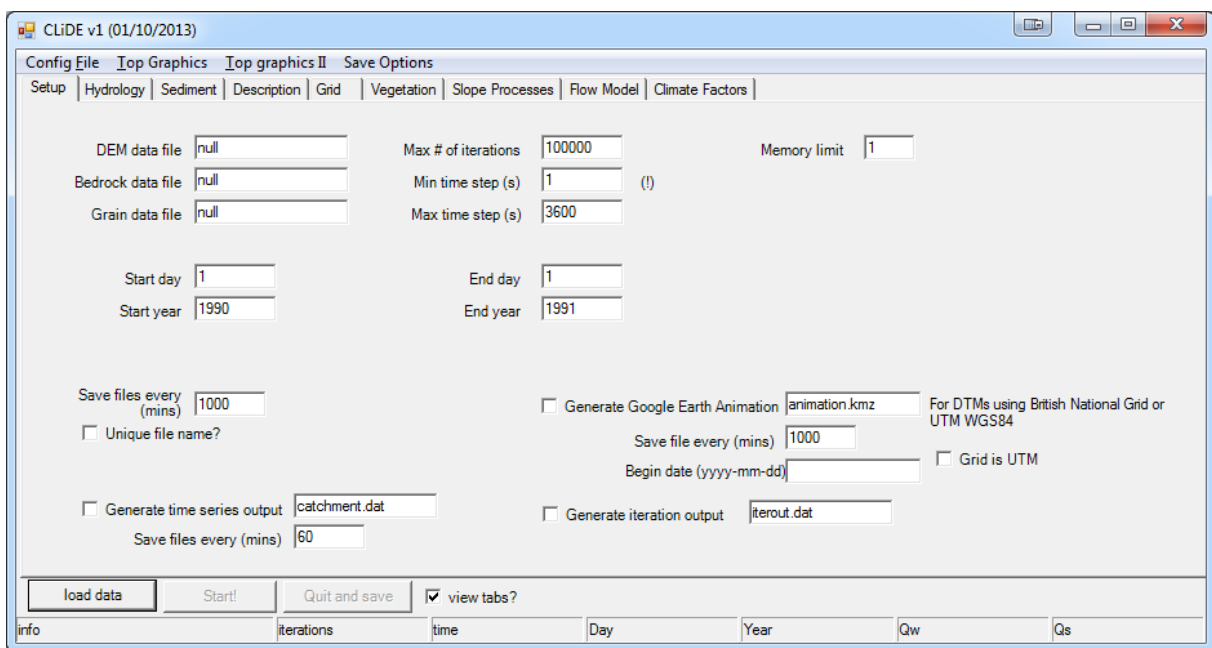


Figure 3 - The CLiDE GUI under the *setup* tab.

When the model has been setup as required, the metadata can be saved as an XML file using the save option in the *Config File* bar. This allows the platform setup to be reproduced at a later time and will save time if multiple similar setups are required.

Populating the CLiDE platform with initial data and forcing factors is executed by clicking the *Load Data* button at the bottom left of the GUI. Upon loading data, the CLiDE platform will check the compatibility of the input files, assess the potential stability of the model and suggest ways to correct the model input.

Following the upload of information to the model, a new GUI page is visible. It is worth noting that the previous page can be accessed but not modified by selecting the *view tabs?* box. Without starting the simulation, the initialisation data can be viewed in graphical form by toggling components on and

off in the upper graphics tabs. If the hydrological components need to be calibrated, the sediment flux processes may be switched off using the relevant tick box before the simulation is started.

Table 2 - The upper tabs available in the GUI and description of their parameters

Tab	Overview
Setup	Allows the DEM, Grain Size and Bedrock Elevation file names to be specified. The temporal settings for the simulation and the output of files are also controlled here.
Hydrology	Specify values or distributed files for the surface water partitioning and groundwater components.
Sediment	Enter the distribution of grain sizes, the scheme to transport sediment and the transport properties.
Description	A description of the simulation can be saved as metadata for future reference.
Grid	Grid settings from the input files can be overridden (not recommended).
Vegetation	The shearing, maturity and erosion characteristics may be modified.
Slope Processes	A general creep rate may be required for longer term simulations. There are three slope failure schemes – a simple sand pile algorithm, the SCIDDICA debris flow model or the SIBERIA sub model.
Flow Model	Controls the LISFLOOD surface flow routing characteristics.
Climate Factors	Allows uniform or a linear climate factor to be applied to the input precipitation and potential evapotranspiration datasets.

To initialise the simulation select the *Start!* button at the bottom left of the GUI. During simulation, the simulated time, number of iterations, and catchment discharged sediment and water can be viewed at the bottom of the GUI. The graphical options in the upper tabs may be switched on and off to view the runtime output from the model. These will be updated at the file save interval, specified before

loading the data into the model (under the *setup* tab), or when the *Update Graphics* button is clicked. The image in the GUI will be saved in the .jpg format, ready for display in Google Earth, if the *Graphic to Google Earth* button is clicked or when specified under the pre-load setup tab.

The simulation may be terminated at any time using the *Quit and save* button, producing output files for the current time-step and shutting down the GUI.

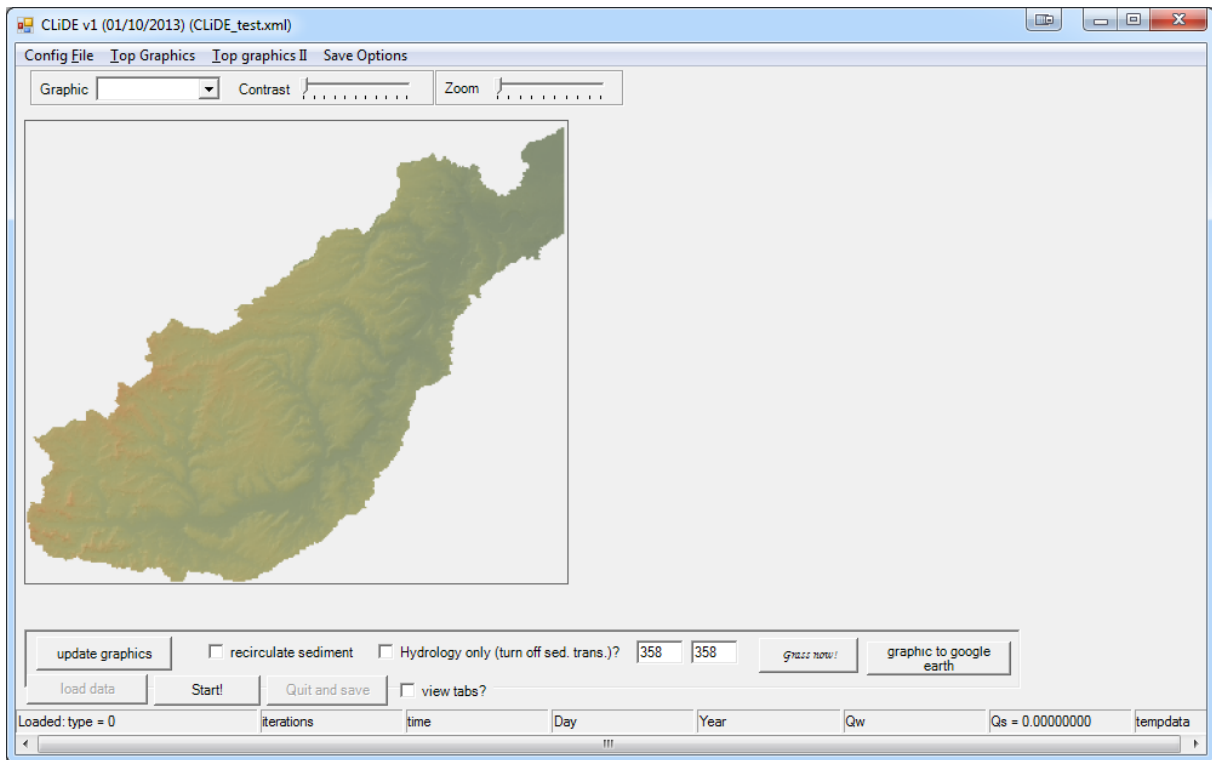


Figure 4 - The GUI after the simulation input data has been loaded into the model

### 3.5 DISCRETISATION

The CLiDE platform will accept any grid cell size (though all cells must be the same size and an integer) and has been used with DEM's from 1 m to 200 m cells. However, choice of grid cell size is important, as there are significant compromises to be made between the area that can be modelled, the resolution, and simulation time. The CLiDE platform can run with up to 2 million grid cells, but is probably best suited to applications with 250,000 to 500,000 cells. Quite simply, the smaller the number of grid cells, the faster the model will operate. This is particularly important, as increasing the resolution linearly, results in an exponential increase in the number of grid cells. Furthermore, the *erodelimit* parameter, which controls the nodal erosion and deposition volume per iteration, can be contingent on grid cell size.



Changes in cell elevation represent changes in local slopes, and a 0.1m change with 1m cells equals a 10% change in slope, yet a 0.1m change in 10m cells equals a 1% change. Thus, increasing the grid cell size of the DEM results in a greater than exponential increase in computational time, as changes between grid cells result in a less severe alterations in slope.

These resolution issues are also contingent upon the time that is required to be modelled. If a single event is to be simulated, then this can be carried out at a higher spatial resolution that may (for example) take a day to run. If 100 years are to be simulated, this period may contain hundreds of events, and so take weeks or months to complete.

There are many ways in which the model speed can be increased, including parallelisation by dividing a catchment into sub catchments and running these sub catchments simultaneously on separate machines. In addition, the cell size affects the time step of the flow model. This time step is controlled by the courant number, flow depth and the grid cell size. Smaller grid cells will lead to smaller time steps, as flow cannot be moved across more than one cell at once. Furthermore, smaller grid cell sizes lead to (as above) greater relative changes in elevation between cells and a smaller courant number may be required in order to maintain numerical stability of the flow model.

Due to the daily input of distributed rainfall and potential evapotranspiration into the CLiDE platform, start and end dates must be specified in the *Setup* tab. The day data is input as day number within the year, for example 23<sup>rd</sup> January would be 23 and 30<sup>th</sup> October would be 303 for a standard year or 304 for a leap year. The start date also needs to be entered into the Google Earth animation section if this output is required. Due to the inclusion of set dates in the CLiDE platform, the maximum number of iterations is irrelevant, however, it must be set at a high enough number not to interfere with the simulation being undertaken.

### **3.5.1 DEM**

The CLiDE will accept a digital elevation model (DEM), to represent the height of the terrain surface above a defined datum, at any uniform discretised size. The DEM used will act as the reference spacing for all other input files unless otherwise specified. Unlike previous versions of CAESAR, on which the CLiDE is based, no pre-processing rotation of the DEM to a particular orientation is required. This rotation was necessary to allow surface water to drain at the right hand edge of the model, but has been superseded by a specified output location in the *hydrological boundary* file (Section 3.6.3). It is suggested that a north orientated DEM is used, as the coordinate system and many of the post-processing tools, such as GIS, rely on this orientation.

The first six lines of the *DEM data* file contain the domain number of columns and rows, its geospatial referencing details, grid sizing and attributes representing no-data. The remaining lines show the daily elevation (m) for each location on the grid, separated by a white space. There also needs to be a white space at the bottom of the file.

### 3.5.2 Bedrock Elevation

Bedrock elevation is referenced to the same datum (usually mAOD or mAMSL) as the DEM. The surface represented by the bedrock elevation depicts the interface between soil/debris with the underlying solid bedrock. The difference between the bedrock elevation and the DEM at a particular point represents the thickness of soil/debris cover. This information is primarily used by the fluvial sediment transport and shallow landslide components to define maximum scouring depth. At the time of writing it is also intended that this interface will be used for the near-surface transport of water in the unsaturated zone as a potential trigger for debris flows. The bedrock elevation can never be greater than the DEM and, if this rule is violated, the model will reduce the thickness of the bedrock elevation to that of the DEM. The *bedrock data* file shares the same characteristics as the *DEM data* file.

### 3.5.3 Grain Data

Grain size data may be entered using either the grain data file method, contained in the *Setup* tab, or manually through the *Sediment* tab (Section 3.10.3). The latter method initialises the model with a laterally and vertically homogeneous sediment. By inputting a *grain data* file, the model may be initialised with a distributed (both vertical and horizontal) sediment grain size dataset. The *grain data* file contains the percentages of each grain size, specified in the *Sediment* tab, for the active layer and each sub-layer, for every node within the model domain. Each line of the grain data file contains the x and y cell location, the index number within the model, the active layer grain size proportions and ten sub-layer grain size proportions. To use the *grain data* file, the average grainsize proportion information must also be entered into the appropriate place under the *Sediment* tab.

There are two options for creating the *grain data* file. Firstly, a simulation could be started with the tab-only data and allowed to run to a steady state (equilibrium) condition; here the model will produce a *grain size output* file, which may be used for a subsequent transient model runs. This method can be time consuming, and any sub-layers that remain non-active will still have the homogeneous initial grain size proportions. The alternative is to use a downloadable windows based program to generate an initial grain size distribution (Coulthard, 2013). To generate the file using this method, the DEM file (Section 3.5.1) and an ascii map (same format as DEM) of up to five sediment types is required.

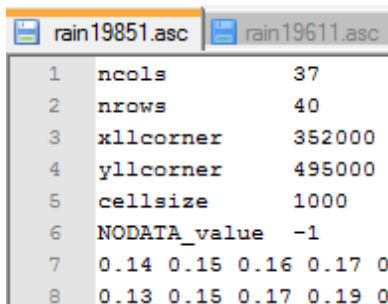
### 3.6 METEOROLOGY

Precipitation and potential evapotranspiration force the model through time, affecting the amount of water in the various stores across the model. Both attributes are distributed, however they have different file format styles due to the way that the data is collated in the UK. The area represented by each meteorological file must be the same as the CLiDE platform boundary.

#### 3.6.1 Rainfall

Rainfall is presented as a gridded ascii file for each day of the simulation. The spatial discretisation of the rainfall files does not have to be the same as the modelled grid, however it must be a factor of the grid spacing. These files must be daily totalled and contained in a folder labelled Rainfall in the same folder as the CLiDE executable. The name of each daily rainfall file has the format *rainYYYYD.asc*, for example *rain19623.asc* and *rain1968321.asc* would represent the daily total rainfall for 3rd January 1962 and 17th November 1968 respectively. A rainfall data file must be present for each day within the simulation, including the extra day in leap years.

The first six lines of each rainfall file contain the number of columns and rows in the rainfall file, their geospatial referencing details, grid sizing and attributes representing no-data (Figure 5). The remaining lines show the daily rainfall (mm d<sup>-1</sup>) for each location on the grid, separated by a white space. There also needs to be a white space at the bottom of the file.



```

rain19851.asc rain19611.asc
1  ncols      37
2  nrows      40
3  xllcorner  352000
4  yllcorner  495000
5  cellsize   1000
6  NODATA_value -1
7  0.14 0.15 0.16 0.17 0
8  0.13 0.15 0.17 0.19 0

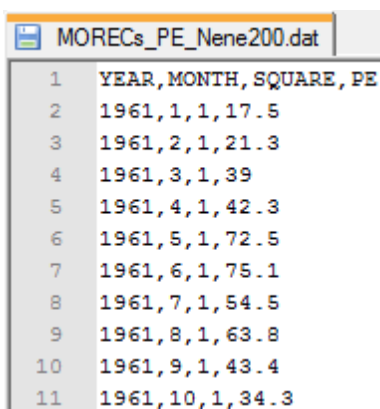
```

Figure 5 - First six lines of a rainfall file, specifying the spatial attributes of the data. The next two lines show the beginning of the dataset (mm d<sup>-1</sup>).

#### 3.6.2 Potential Evapotranspiration

The three files needed to represent monthly averaged potential evapotranspiration are specified under the *Hydrology* tab. The file system is designed for use with the Meteorological Office Rainfall and Evapotranspiration Calculation System) MORECS (Hough and Jones, 1997), although the CLiDE system can be populated with other data.

The *PE grid* file consists of a single distributed ascii file, where individual nodes contain an identifier, which for the MORECS dataset is related to UK evaporation stations. The gridded file has to use the same discretisation as the CLiDE platform. The first six lines of the gridded file contains; the number of data columns and rows in the file, their geospatial referencing details, grid sizing and a no-data value. The grid file links to the *PE List* file, which contains a list of time stamped, monthly averaged potential evapotranspiration ( $\text{kg m}^{-2}\text{s}^{-1}$ ) values for each of the identifiers (Figure 6). As the MORECS dataset is valid for the whole of the UK, the time stamped dataset contains unnecessary data. To reduce the computational cost of reading all the data from the time-stamped file, the third potential evapotranspiration file (*PE Numbers* file) required by the CLiDE contains a list of the PE identifiers required from the *PE List* file (Figure 7) by the *PE grid* file.

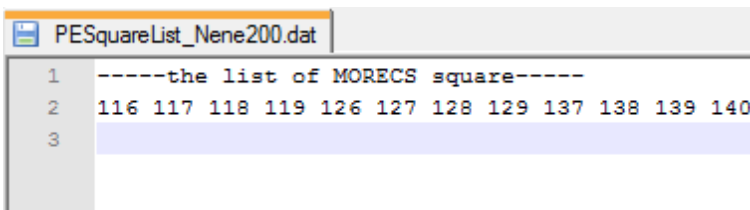


```

1 YEAR, MONTH, SQUARE, PE
2 1961, 1, 1, 17.5
3 1961, 2, 1, 21.3
4 1961, 3, 1, 39
5 1961, 4, 1, 42.3
6 1961, 5, 1, 72.5
7 1961, 6, 1, 75.1
8 1961, 7, 1, 54.5
9 1961, 8, 1, 63.8
10 1961, 9, 1, 43.4
11 1961, 10, 1, 34.3

```

Figure 6 - An example of a PE List file. The first line is a header, and the remaining lines comma-separated, time-stamped, potential evapotranspiration ( $\text{kg m}^{-2}\text{s}^{-1}$ ) data for each identifier over the length of the simulation.



```

1 -----the list of MORECS square-----
2 116 117 118 119 126 127 128 129 137 138 139 140
3

```

Figure 7 - The PE Numbers file contains a list of the identifiers used in the PE gridded file. The first line is a header and the second a white-space separated list of identifiers.

### 3.6.3 Hydrological Boundary

The *Hydrological Boundary* file allows the surface water and groundwater boundary conditions to be specified. The first six lines of the file contain the number of columns and rows in the *Hydrological Boundary* file, its geospatial referencing details, grid sizing and attributes representing no-data. The remaining lines show a two digit number representing the boundary type for each location on the grid. The first digit of the boundary number specifies the groundwater boundary type and the second the

surface water boundary type. Table 3 shows the boundary condition numbers and type. For example 12 would be a no-flow groundwater boundary with a river outflow at the surface.

Table 3 - Hydrological boundary conditions for the CLiDE platform. \*Numbers have been reserved for this boundary type but it has not yet been implemented in the model code.

Boundary Number	Groundwater	Surface Water
1	No-flow or internal node	No-flow or internal node
2	Static specified head node	River outflow node
3*	Static in/outflow node	-
4*	Time variable specified head node	-
5*	Time variable in/outflow node	-
88	Internal fixed debris depth in SCIDDICA landslide module	
-9999	No data (outside catchment domain)	

### 3.6.4 Water Balance

By checking the *Daily Water Balance* box, a water balance file is produced that is updated on a daily basis. This file contains the all of the external fluxes of water ( $m^3 d^{-1}$ ), the amount of water contained within each store ( $m^3 d^{-1}$ ) and the amount that has been passed between stores during that timestep ( $m^3 d^{-1}$ ). The water balance information may be used during the calibration process or to assess the model output.

### 3.7 SURFACE PARTITIONING

The links to the data that describe the soil hydrological characteristics are contained within the Hydrology tab. They are all distributed ascii files, with the same discretisation as the CLiDE Hydrological boundary file. The first six lines of each data file contain the number of columns and rows in the rainfall file, their geospatial referencing details, grid sizing and attributes representing no-data (the same as Figure 5). No-data nodes within these files should define the same the model boundary as for groundwater (see 3.6.3), without the associated conditions.

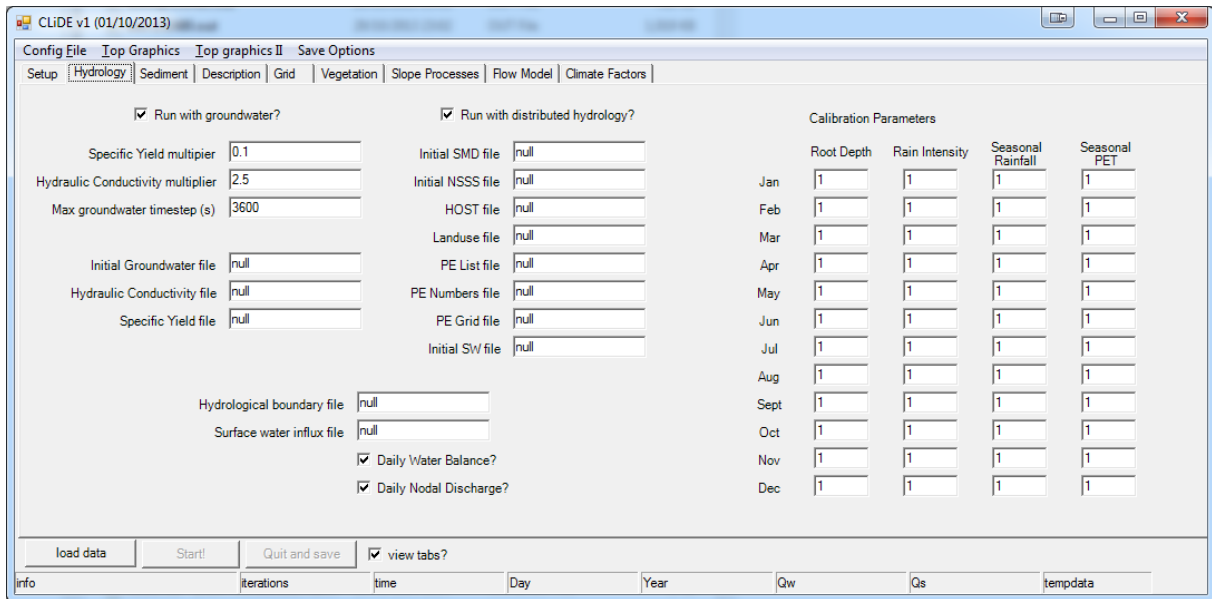


Figure 8 - Hydrological tab parameters in the GUI

### 3.7.1 Soil Moisture Deficit (SMD)

The *Initial SMD* file allows the hydrological model to be initialised from a steady state condition. The initial SMD (mm) can be determined by starting with values of zero, running the hydrological model to steady state, and using the final SMD output as an input for the transient run. This process may form part of the calibration process (see Section 5).

### 3.7.2 Near Surface Soil Storage (NSSS)

The *Initial NSSS* file allows the hydrological model to be initialised from a steady state condition. The initial NSSS (mm) can be determined by starting with values of zero, running the hydrological model to steady state, and using the final NSSS output as an input for the transient run. This process may form part of the calibration process (see Section 5).

### 3.7.3 Landuse

Landuse divides the model domain based on vegetation properties at each node in the data array based on 10 class types (Morton et al. (2011)). The Landuse file provides the surface partitioning model SLiM with the rooting depth (m), depletion factor (-) and crop coefficient (-) for each landuse class. Rooting depth is defined as the maximum depth of root penetration for a particular vegetation type. Depletion factor and the crop coefficient take into account the influencing conditions under which evapotranspiration is determined for vegetation classes.

Table 4 – Landuse habitat numbers and associated descriptions (Morton et al., 2011).

Landuse Number	Habitat Description
1	<b>Broadleaf woodland</b> <i>Broadleaved, Mixed and Yew Woodland</i>
2	<b>Coniferous woodland</b>
3	<b>Arable</b> <i>Arable and Horticulture</i>
4	<b>Improved grassland</b>
5	<b>Semi-natural grassland</b> <i>Rough Grassland Rough grassland</i> <i>Neutral Grassland</i> <i>Calcareous</i> <i>Grassland</i> <i>Calcareous</i> <i>Grassland</i> <i>Acid Grassland</i> <i>Fen, Marsh and Swamp</i>
6	<b>Mountain, heath, bog</b> <i>Dwarf Shrub Heath</i> <i>Heather</i> <i>Heather grassland</i> <i>Bog</i> <i>Montane Habitats</i> <i>Inland Rock</i>
7	<b>Saltwater</b>
8	<b>Freshwater</b>
9	<b>Coastal</b> <i>Supra-littoral Rock</i> <i>Supra-littoral</i> <i>Sediment</i> <i>Supra-littoral</i> <i>Sediment</i> <i>Littoral Rock</i> <i>Littoral Sediment</i>
10	<b>Built-up areas and gardens</b>

### 3.7.4 Hydrology Of Soil Type (HOST)

The *HOST* file allows further vegetation and soil hydrological properties to be defined, and is composed of 31 different classes (Boorman et al., 1995) as defined in the input file. Each class has a known field capacity (m), wilting point (m) and baseflow index (-). Field capacity describes the maximum amount of water that the soil can hold and wilting point the minimum soil moisture a particular vegetation class requires not to wilt. The soil baseflow index (between 0 and 1) determines the partitioning ratio between groundwater recharge and surface runoff under conditions of excess water for each HOST soil class. Under high BFI values greater proportion of excess surface water is

passed on as recharge. As BFI approaches zero, a greater proportion of excess surface water is partitioned as runoff. The HOST datasets work in conjunction with the Landuse dataset described in Section 3.7.3.

Table 5 – Definition of the 29 HOST soil class numbers (modified from Boorman et al., 1995). The remaining two classes (30 and 31) are used to describe surface water features. The integrated air capacity (IAC - is the average percentage air volume over a depth of one metre) is used to differentiate some classes.

Substrate Hydrology	Mineral Soils				Peat Soils	
	Groundwater	No impermeable or gleyed layer within 1m	Impermeable layer with 1m or gleyed layer at 0.4-1m	Gleyed layer within 0.4m		
Weakly consolidated, microporous, by-pass flow uncommon (chalk)	Normally present at >2m	1				
Weakly consolidated, microporous, by-pass flow uncommon (limestone),		2				
Weakly consolidated, macroporous, by-pass flow uncommon		3	13	14	15	
Strongly consolidated, non- or slightly-porous, by-pass flow common		4				
Unconsolidated, macroporous, by-pass flow very uncommon		5				
Unconsolidated, microporous, by-pass flow common		6				
Unconsolidated, macroporous, by-pass flow very uncommon	Normally present at ≤ 2m	7		IAC <12.5	IAC ≥12.5	Drained
Unconsolidated, macroporous, by-pass flow very uncommon		8		9	10	11
Slowly permeable	No significant groundwater	16	IAC >7.5	IAC ≤7.5	24	26
			18	21		
Impermeable (hard)		17	19	22		27
Impermeable (soft)			20	23	25	
Eroded peat						28
Raw peat						29

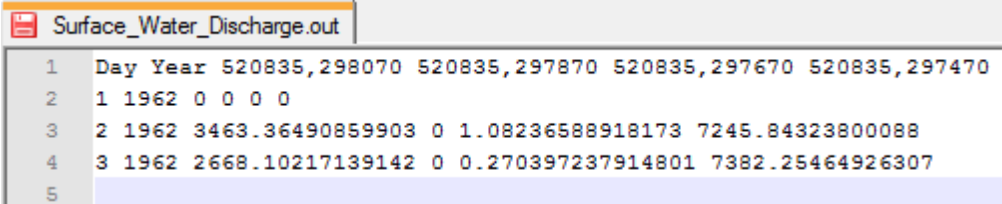


### 3.7.5 Initial Surface Water

The *Initial surface water depth* file allows the hydrological model to be initialised from a previous condition and can reduce model spin-up time. Surface water depth (m) can be initialised either; by entering the file name 'null', whereby all values will be zero and a long spin-up time will be required or by taking a previously saved *waterdepth.##.out* file, renaming and initialising from these water depths. This process may form part of the calibration process (see Section 5).

### 3.7.6 External Surface Water IOs

Surface outflow from the boundary of the model at specified location (Section 3.6.3) can be recorded by checking the *nodal discharge* box. The output file, *Surface\_Water\_Discharge.out*, logs the daily water discharge ( $\text{m}^3 \text{d}^{-1}$ ) from each node and gives the coordinates for each point. The inclusion of a *surface water influx* file allows a time series of surface water to be added to any nodes within the model boundary. The *surface water influx* file takes the same format as the *surface discharge* file, allowing the output from one subcatchment to act as the input for the next subcatchment.



	Day	Year	520835,298070	520835,297870	520835,297670	520835,297470
1	1	1962	0	0	0	0
3	2	1962	3463.36490859903	0	1.08236588918173	7245.84323800088
4	3	1962	2668.10217139142	0	0.270397237914801	7382.25464926307
5						

Figure 9 - Example surface water discharge file. The first line defines the coordinates of the outflow nodes and the following line the daily water outflow ( $\text{m}^3$ ) from that node.

## 3.8 GROUNDWATER

Groundwater is linked to the surface water routing model Lisflood through baseflow return to rivers, and to the SLiM water partitioning code by the daily recharge that it receives. Spatially the groundwater module is discretised at the same scale as the *hydrological boundary* file. The module has a timestep that is uniform over a day but that can vary on differing days based on the domain maximum cell Reynolds number. If the maximum domain Reynolds number approaches one, the number of time steps within a day is increased until a more stable setup is found. The groundwater module is initialised using groundwater head levels and constrained by the hydraulic conductivity and specific yield of the aquifer. These constraints may be specified as either uniform for the entire catchment or as distributed using ascii files. The groundwater module may be disabled to aid

calibration of the surface hydrological components. Under these conditions recharge continues to be removed from the surface water store, however, baseflow is no longer returned to rivers.

### 3.8.1 Initial Groundwater

The *Initial groundwater* file allows the hydrological model to be initialised from a steady state condition. If initial groundwater levels (mAOD or mASL) can not be determined from other sources, they may be found by setting initial values to the same as the DEM and letting the model relax to a balance point. Following this model spin-up stage, or if initial groundwater levels are known, future transient runs may be initialised. This process may form part of the calibration process (see Section 5).

### 3.8.2 Hydraulic Conductivity

The aquifer hydraulic conductivity ( $\text{m d}^{-1}$ ) must be specified as either uniform or distributed. To set a uniform value across the domain, enter the required value in the *Hydraulic Conductivity Multiplier* box and leave the *Hydraulic Conductivity* file name as 'null'. For a spatially distributed hydraulic conductivity, a gridded ascii file with header information is required in the same format as the *Hydrology boundary* file. If a distributed hydraulic conductivity file is used, the *Hydraulic Conductivity Multiplier* box allows every value to be scaled by the number in the box. For example, '2' would double the hydraulic conductivities as specified in the file and '0.25' would quarter the values. This value must be positive and if no scaling is required, then it must be set to '1'. The scaling factor may be useful in determining hydraulic conductivity during the calibration process (see Section 5).

### 3.8.3 Specific Yield

The aquifer specific yield (-) is set using the same method as hydraulic conductivity and must be specified as either uniform or distributed. To set a uniform value across the domain, enter the required value (0 - 1) in the *Specific Yield Multiplier* box and leave the *Specific Yield* file name as 'null'. For a spatially distributed specific yield, a gridded ascii file with header information is required in the same format as the *Hydrology boundary* file. If a distributed specific file is used, the *Specific Yield Multiplier* box allows every value to be scaled by the number in the box. For example, '2' would double the specific yield as specified in the file and '0.25' would quarter the values. This value must be positive and if no scaling is required, then it must be set to '1'. The scaling factor may be useful in determining specific yield during the calibration process (see Section 5). Specific yield is limited to unity and therefore any values greater than this will be reduced to one without producing any warnings.

### 3.9 LISFLOOD SURFACE FLOW

Following the daily partitioning of surface water by the SLiM module, and calculation of baseflow return to rivers by the groundwater module, Lisflood controls the surface routing of water around the domain using a variable timestep based on domain maximum water depth. The calculated daily addition or removal of water by SLiM and the groundwater module are discretised at the timestep used by Lisflood. Lisflood takes slope, water depth, and surface frictional characteristics into account whilst distributing water around the catchment.

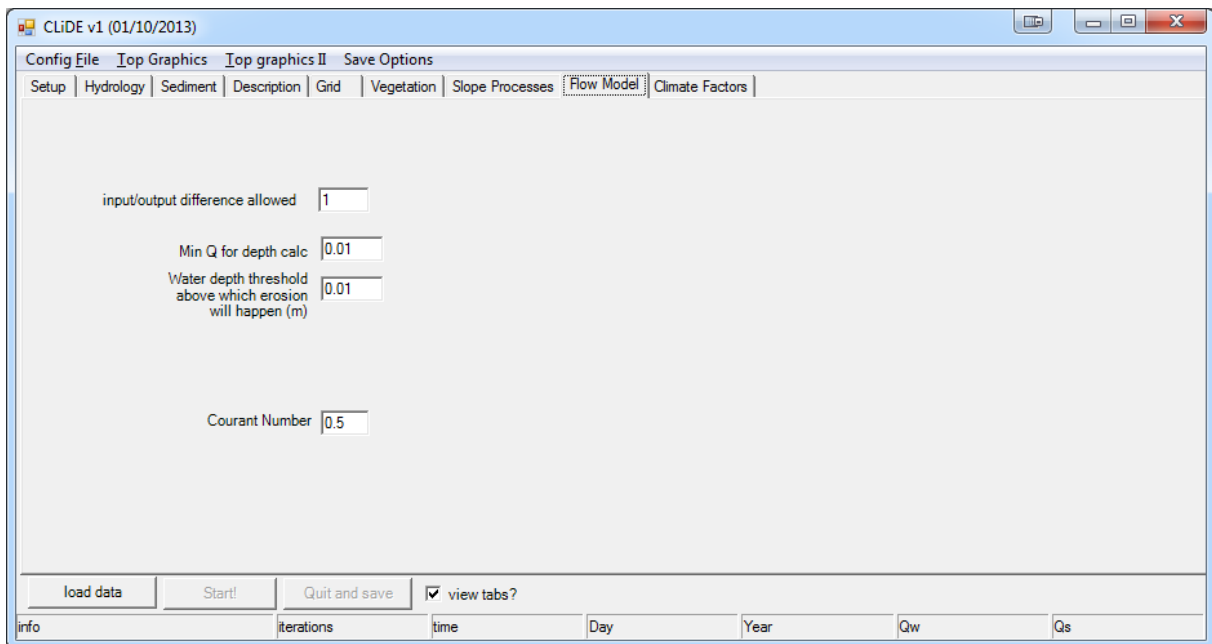


Figure 10 - Flow model (Lisflood) tab parameters in the GUI

#### 3.9.1 Input - output difference

The *Input - output difference allowed* option (Figure 10) allows the speed of platform operation to be increased. CLiDE calculates surface water discharge from the catchment boundary and, if this is equal to that being added by SLiM and through baseflow return, we assume the flow model is running in a steady state. If so, we can detach the time step of the flow model from that of the erosion and deposition model and allow the time steps to extend to that determined by erosion and deposition. The value of *Input - output difference allowed* is the difference in cumecs between the input and output that is acceptable to allow the model to run in this faster mode. It is sensible to set this value close to the low flow value or mean annual flow. The CLiDE platform will shift automatically between the two states of operation.

### 3.9.2 Min Q and Water Depth Threshold

The *Min Q for depth calc* box (Figure 10) defines a threshold above which the CLiDE platform will search for the domain maximum flow depth that determines the time stepping attributes. If this is set too low, computing resources are wasted calculating sub-millimetric flow depths, which will not result in erosion or deposition. The variable is dependent upon grid cell size and as a guide is set to a 100<sup>th</sup> of cell width, for example; a DTM with 10m cell size will have a Min Q of 0.1, and a DTM with 50m cell size will have a Min Q of 0.5. The flow depth (m) above which CLiDE calculates erosion can be set under the *Flow Model* tab. The standard value is set to 0.01 m, however lower values can be used on very high resolution DEM's and larger values on large grid cell widths (> 50m).

### 3.9.3 Courant Number

The Courant number ((Figure 10) is a value that controls the numerical stability and operation speed of Lisflood. More details can be found in Bates et al. (2008). The Courant number should only range between 0.2 and 0.7, where higher values increase the model time step but are more unstable. Stability, and thus coefficient values, depend upon the grid cell size. Larger cells widths (> 50 m) can take values of 0.7, smaller cell widths (< 2 m) may need the smallest value (0.2). Stability is also linked to the *erodelimit* value, which controls the amount of sediment that can be eroded or deposited from a cell during a timestep.

## 3.10 SEDIMENT

A range of options are available for the representation of initial sediment grain size proportions, transport and erosion properties. The grain size (m) and proportion (as a fraction of 1) columns allow the initial grains size properties to be assigned. The distribution of these sizes is considered homogeneous both vertically and horizontally across the domain. If a *Grain data* file (Section 3.5.3) is used to initialise grain size distribution, a more heterogeneous distribution can be achieved. As a simulation progresses, the sediment grain sizes are distributed across the catchment.

### 3.10.1 Fall Velocity and Transport Method

The CLiDE platform retains the two methods of fluvial sediment transport used by CAESAR where a flow depth exists. The Einstein-Brown method can be used for a single grainsize and the Wilcock and Crowe formulation for up to 9 different grainsizes. The *suspended sediment* check box (Figure 11) allows sediment grain sizes at the value specified in the *size1* box, to be treated as suspended. The fall flow velocity for these grains may be specified in the *fall velocity* box ( $\text{m s}^{-1}$ ).

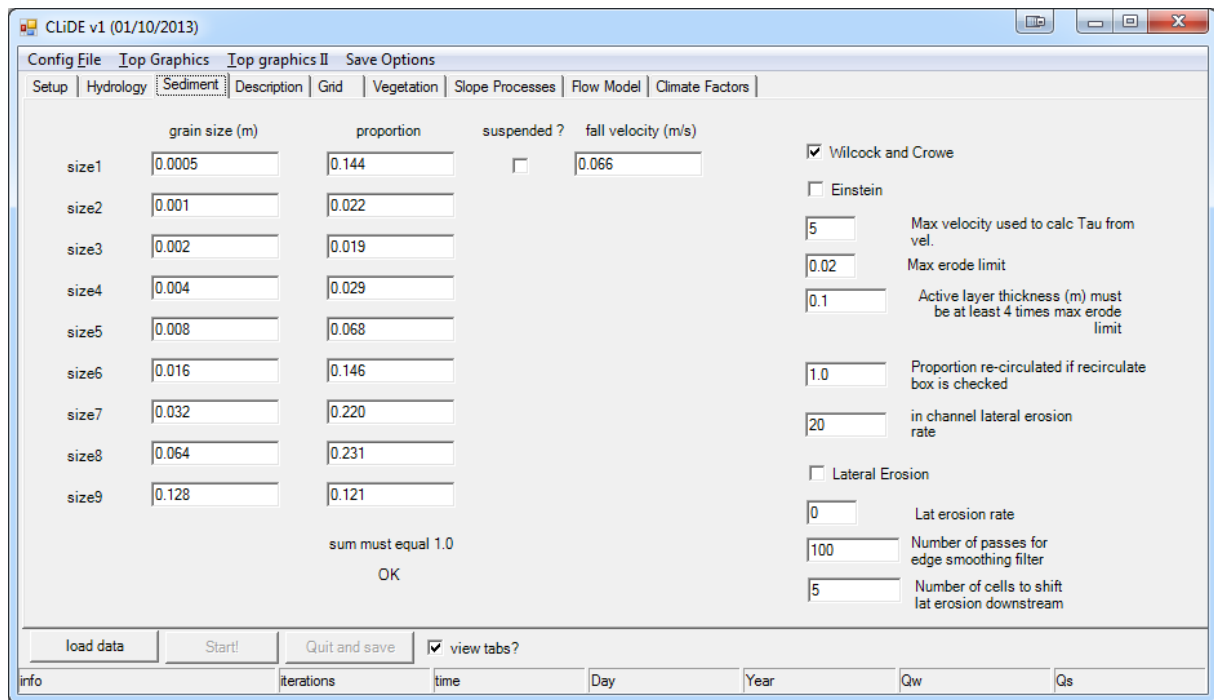


Figure 11 - Sediment tab parameters in the GUI

### 3.10.2 Max Velocity and Max Erode Limit

Where steep gradients exist between cells in the DEM, a value can be set for the maximum velocity ( $\text{m s}^{-1}$ ) used to calculate sediment transport. A *max erode limit* (Figure 11) may also be imposed to define the maximum amount of material that can be eroded or deposited within a cell. This parameter prevents numerical instability caused by too much material being moved from cell to cell. The *max erode limit* also controls the time step, which is restricted to allow this value (as a maximum) to be moved from one cell to another.

### 3.10.3 Active Layers

Sediment transport occurs using a series of active layers. Below these active layers a series of non-active subsurface layers exist, allowing development of a limited stratigraphy. Erosion and deposition of sediment occurs in the active layer at the surface. If deposition occurs and the thickness of the active layer exceeds 150% of the depth (m) specified in the *Active layer thickness* box (Figure 11), the specified depth of active layer is archived in the topmost subsurface layer and the active layer is reduced in depth by 67%. When this occurs, the grain size record in each subsurface layer is passed to the layer directly below. Where erosion occurs and the active layer thickness is below 25% of the depth (m) specified in the *Active layer thickness* box, the topmost subsurface layer depth, and its grain size record, is incorporated into the active layer. Within the active layer and each subsurface

layer, grain size distribution is assumed to be homogeneous at the cell scale. In order to maintain stability, the active layer thickness specified must be at least four times the *max erode limit*.

### 3.10.4 In Channel Lateral Erosion

The *in channel lateral erosion rate* (Figure 11) controls channel width by setting the sediment cohesion properties. Sediment that is loosely packed and unconsolidated is represented by a higher value, and can be readily eroded and laterally transported (within the channel) resulting in a shallow wide channel. If it is more cohesive (represented by a lower value), it is harder to move laterally then a narrower deeper channel results. The *in channel lateral erosion rate* is required to reduce the positive feedback exhibited where erosion focuses more flow on that cell, which causes increased erosion, leading to single thread deep channels. Initial values of between 10 and 20 are recommended for most river types.

### 3.10.5 General Lateral Erosion and Rate

The *lateral erosion* check box (Figure 11) determines whether bank erosion can occur within the platform. The *lateral erosion rate* is calculated by the radius of curvature, which is done according to the edge counting method described in Coulthard and Van de Wiel (2007):

$$\text{rate of lowering of bank cell} = (1/Ca) \times \text{Tau} \times \text{LateralErosionRate} \times \text{Time}$$

Where *Ca* is radius of bend curvature (m), *Tau* is the shear stress of the cell adjacent to the bank, lateral erosion is the specified rate and time is in seconds. Material removed from the bank cell is added to the cell adjacent to the bank. Lateral erosion only occurs for 4 orthogonal neighbouring cells. Values for this parameter need to be derived through calibration as each catchment is unique. Following experimentation a *lat erosion rate* of between 0.01 and 0.001, seems adequate for braided rivers, and a *lat erosion rate* around 0.0001 for meandering channels or channels with little lateral erosion. This value is grid cell independent, so rates of erosion for the same site on a 20m DEM should be the same for a 50m DEM.

### 3.10.6 Number of Passes and Cell Shifting

The *number of passes for edge smoothing filter* value (Figure 11) describes how smooth the calculated curvature of the channels is. Values calculated by this method can be displayed when the model is running with the *lateral gradient display* option (Section 4.4.2). This will show red for the outside of bends and green for the inside. As a rough guide, this value should be set as the frequency of meanders (or distance between two meanders) in grid cell size. Too small a number will result in

lumpy lateral development, too large will result in too little movement and smoothing across bends. The edge gradient that the CLiDE platform uses to determine lateral erosion can be shifted downstream. This allows meander bends and bars to migrate downstream. Suggested values are around 10% of the values used for the above number of passes for edge soothing filter (typical values ranges from one to five). Both the number of passes and shifted number of cells need to be integers.

### 3.11 VEGETATION

The *Vegetation* tab contains parameters relating to vegetation parameterisation within the CLiDE platform. Vegetation parameters under this tab restrict sediment erosion and surface water flow rates and are not currently linked to the vegetation properties in the SLiM water partitioning or the SCIDDICA shallow landslide modules.

The *vegetation critical shear* is the shear stress value, imparted by water flow, above which vegetation will be removed by fluvial erosion. Low values allow vegetation to be swept away easily and higher values result in a more resistant vegetation.

*Grass maturity* defines the time taken (in years) for vegetation to reach full maturity, with greater maturity reducing erosion rates. The proportion of erosion that can occur when vegetation reaches fully grown (0 to 1) determines how vegetation maturity affects the *in channel lateral erosion* and general *lateral erosion* rates (Section 3.10.5). If set to 0 then, when fully grown, there can be no erosion using these two methods and if set to 1, then vegetation will have no affect on erosion. If set to 0.5, then when vegetation is fully grown 50% of normal erosion by channel and general lateral erosion will be allowed. However, this rate is affected by the level of maturity, so if the vegetation is 50% mature and the proportion of erosion is 0.5, the maximum allowable amount of erosion will be 0.75 of the no vegetation rate.

### 3.12 SLOPE PROCESSES

This tab contains the parameters used to control non-fluvial sediment transport processes within the CLiDE platform. *Creep* rate and *Soil erosion* rate (Figure 12) allow the impacts of decadal and centennial scale processes to be included in the landscape evolution aspect of the platform. Shallow landsliding events can also be captured using either a simple sand pile model, which uses slope angle to trigger landslides, or by a more complex system that also takes soil properties, friction, adhesion and momentum into account.

### 3.12.1 Creep and Soil Erosion Rates

Soil creep is represented using a simple diffusive function defined by equation 2.18. The function will tend to create erosion on steeper slopes, and to round off of sharper features in the terrain. Typical values are 0.0025. The soil erosion function is an adaptation of USLE type approaches, where soil erosion is a function of the slope length, slope and a series of coefficients. Notably the slope length is derived by the square root of the drainage area at a point. There are no suggested values for this function, and it has not been calibrated or tested against field data to date.

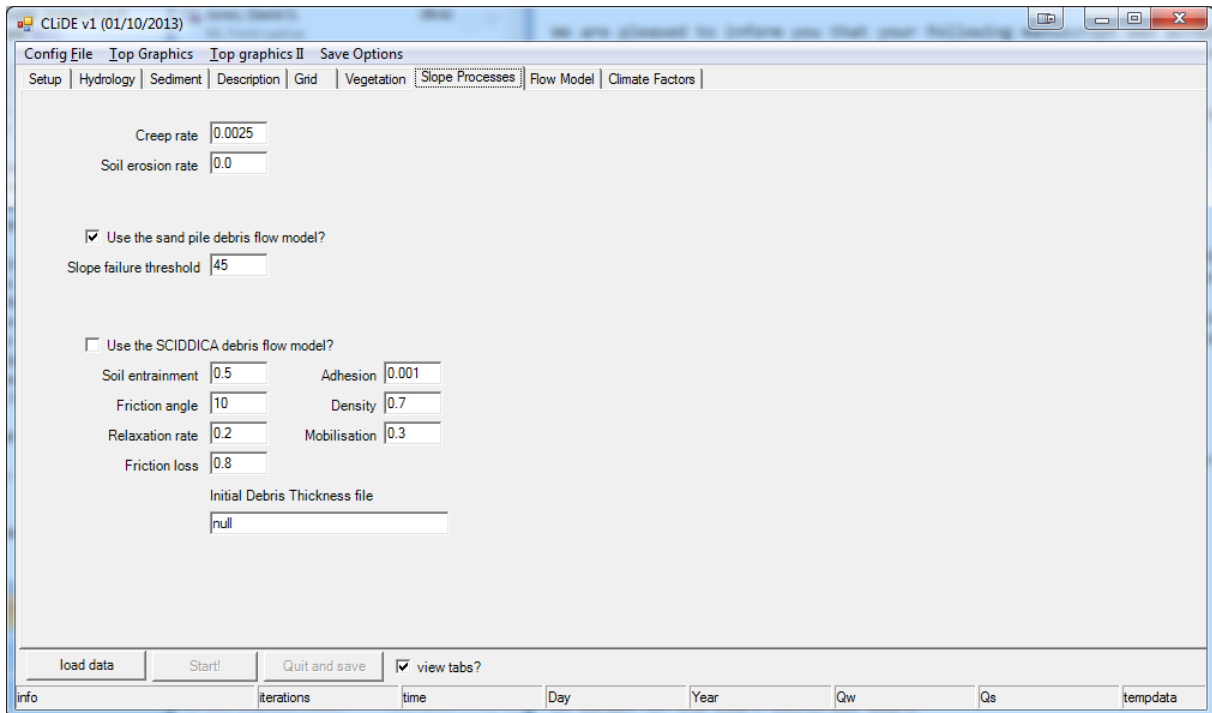


Figure 12 - Slope Process tab parameters in the GUI

### 3.12.2 Sand Pile

A simple sand pile function (Figure 12) can be used to generate shallow translational landslide events, which are triggered when the slope angle between two or more cells is greater than the stated threshold. The sand pile algorithm is similar to that described by Metha and Barker (1994) and can be triggered either by erosion at a slope base or by the addition of sediment to the slope top. Both of these processes allow the *slope failure threshold* angle to be exceeded and sediment to be passed between cells. The passing of sediment between two cells often leads to a cascade effect that can influence many cells. Non-fluvial movement of sediment as shallow landsliding is considered instantaneous within the model framework.



### 3.12.3 SCIDDICA

SCIDDICA allows for a more advanced representation of shallow translational landslide processes in comparison to the simpler sand pile method. The module calculates the potential energy contained within each cell based on the volume, weight and momentum of material. Like the sand pile model, SCIDDICA may be triggered by a change in slope between cells that exceeds a threshold value, however, it may also be triggered by the evolving hydrological properties at the surface or within the soil layer. Many of the SCIDDICA variables can be determined through calibration. Currently all factors are homogeneous across the catchment.

#### SOIL ENTRAINMENT

Along the landslide path, soil may be entrained into the landslide material, adding mass to the flow. The *Soil entrainment* coefficient (0 to 1) determines the maximum percentage of available soil material that may be entrained into a particular landslide event. The higher the coefficient, the greater the volume of soil material available for entrainment.

#### FRICITION ANGLE

The *Friction angle* ( $0^\circ$  to  $90^\circ$ ) is a threshold value similar to the slope failure threshold (Section 3.12.2), which determines the minimum slope angle between cells over which a landslide can occur. Unlike the slope failure threshold angle, not all inter-cell slopes above this angle will fail as failure is determined by several factors including the landslide run-up; the additional landslide thickness produced by the drop in overall density when under momentum. A greater friction angle reduces the number of landslides within the domain.

#### RELAXATION RATE

The *Relaxation rate* coefficient (0 to 1) determines how many internal time steps are undertaken per simulated timestep. This avoids instability within the module, whilst maintaining efficiency. The relaxation rate must take into account cell size and the duration of each internal time step. The lower the coefficient, the greater the number of time steps used by the module to reach a balanced condition. If this value is too high, numerical instability may occur, and if set too low, computational resources are wasted.

#### ADHESION

Defines the minimum depth (m) of loose material that will remain following a debris flow.

#### DENSITY

The density ( $\text{g cm}^{-3}$ ) of the soil above the bedrock surface.

## MOBILISATION

Within SCIDDICA, the mobilisation of loose soil cover occurs when a landslide entrains and mobilises the subsurface soil cover. A certain amount of energy is required within the landslide to entrain the soil and this threshold is set using the mobilisation coefficient. The lower the value ( $m^3$ ) the easier it is for soil to be entrained into the landslide.

## FRICITION LOSS

The *Friction loss* parameter (m) accounts for the loss of energy through frictional processes at the landslide-surface interface. Within the model this parameter acts as the limit to which run-up thickness may reach and thus removes some of the energy from the system if run-up tries to exceed this limit.

## INITIAL DEBRIS THICKNESS

A gridded ascii file containing the thickness of surface debris (m), where the first six lines of the contain, the number of data columns and rows in the file, their geospatial referencing details, grid sizing and no-data value. The remainder of the file contains the thickness information discretised at the same spatial scale as the CLiDE boundary file. The values within this file must be equal to or less than the soil depth.

### 3.13 CLIMATE FACTORS

The Climate factors allow the input rainfall (PPTN) and potential evapotranspiration (PE) files to be perturbed in order to simulate the impacts of climate change. Both inputs may be perturbed on a monthly basis and the value entered each month represents a multiplication factor. For example, a value of 2 entered for January PPTN will double all input rainfall and a value of 0.5 will reduce the input rainfall by half. The perturbation is applied evenly throughout the simulation unless the linear CF application box is checked. If this box is checked, the perturbation is applied linearly over the duration of the simulation, starting with no change and ending with the full perturbation being applied.

## 4 CLiDE Model

### 4.1 INTRODUCTION

This section details the process of running a simulation using the CLiDE platform, from initialisation to the file output stage. Post processing is discussed in the next section (Section 6). The CLiDE platform may be used to simulate either real or idealised data cases using similar methods.

### 4.2 INITIALISATION

The platform is initialised using the input data described in Section 3. It is important that these files are, where necessary, consistent with each other and share the same grid information. Once the platform has been setup with the required data, an XML of the initialisation data may be saved under the *Config File* tab. By saving an XML of the initialisation data, future simulations may be initialised using the same files without having to re-enter the file name information or parameter values. An XML file from a previous simulation may be loaded by accessing the *Open* option under the *Config File* tab.

Once the correct data has been selected in the GUI, it can be loaded into the model using the *load data* button. Whilst loading the data, CLiDE checks the input datasets and parameters for consistency and flags errors. The error flags warn of possible errors and provide a solution for rectification. To rectify these errors the platform must be shut down and restarted. Not all errors will provide a flag during this process, it is therefore important to check that the model is running correctly and producing the expected output files (see Section 6).

Upon initialising the platform data, the simulation may be started by clicking the *Start!* button. If the platform is running, the iteration and time counters in the bottom of the GUI window will count up. The bottom left panel will also say what module the CLiDE platform is processing at the current time.

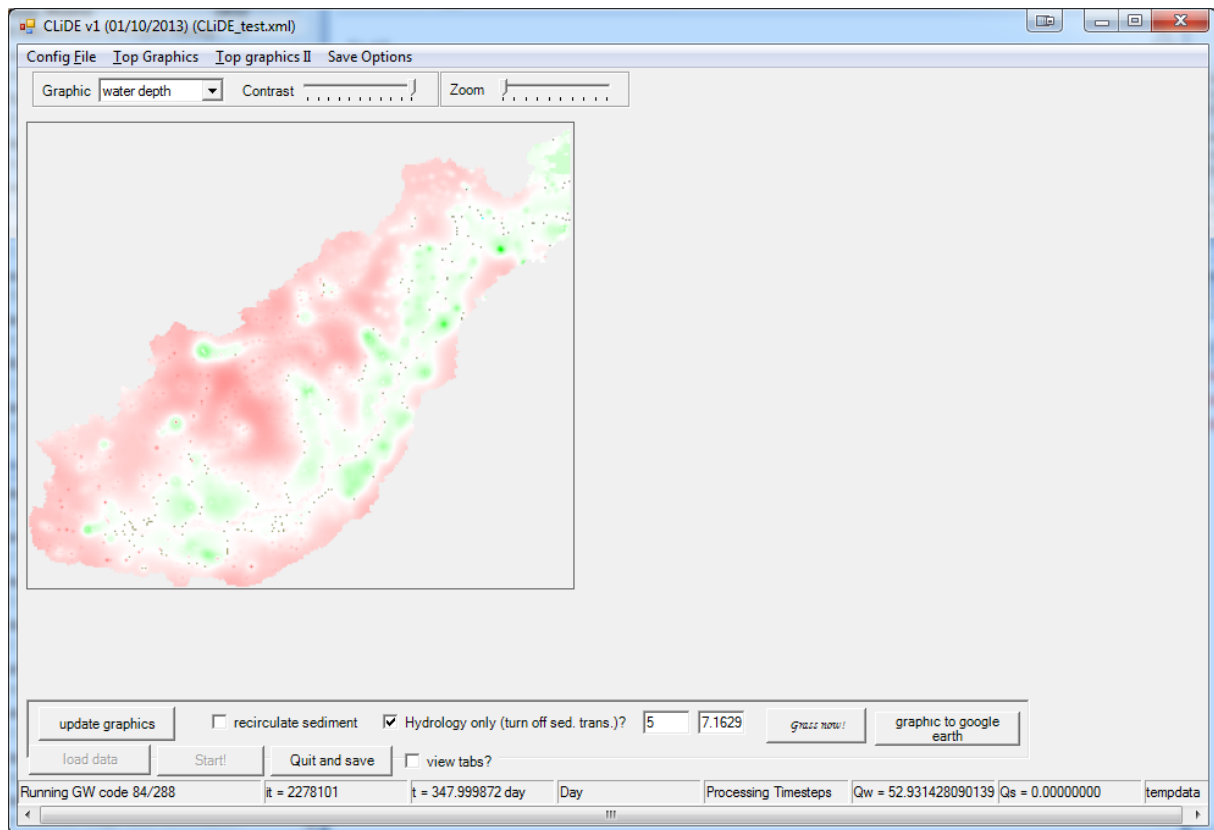


Figure 13 - Snapshot of the CLiDE GUI displaying changes to groundwater levels after 348 days of simulation

### 4.3 RUNTIME

During runtime several options are available including graphical, file saving and runtime options. The former two are described in Sections 4.4 and 4.5. The runtime options allow the sediment transport module to be switched off whilst the model is running (via the *Hydrology only* tab (Figure 13)). This reduces the required computational resources and therefore the runtime. This option is useful during the hydrological calibration stage of the simulation process, as sediment transport rates are not required. The other option available during runtime is to *Grass now!* (Figure 13). This option instantly provides vegetation to the areas adjacent to water flow paths within the model.

In addition to the time and iteration information displayed at the bottom of the GUI window the  $Q_w$  panel indicates the volume of water ( $m^3$ ) removed from the domain by river flow during the previous iteration and  $Q_s$  the volume of bedload sediment removed from the domain during the previous daily timestep (only available when erosion/deposition enabled in graphical options).

At any point within a simulation, the run may be terminated using the *Quit and save* button at the bottom of the GUI.

## 4.4 SAVE OPTIONS

There are three types of data that can be saved during simulation. Time series files are continuously updated during the simulation and consist of one, usually large, file with limited spatial information. The remaining two save options capture data at a single point in time, either as graphical or ascii gridded formats, creating multiple smaller files at equally spaced intervals. The saving of files is controlled by both the set of options that are contained within the *Setup* tab (Section 3.4) and those in the Save Options bar at the top of the GUI (Figure 13).

### 4.4.1 Time Series

The *generate time series output* option in the *Setup* tab (Figure 3) creates a single time series file (name specified in relevant box) of: time (mins), the water discharged from the system (cumecs), the catchment volume of rainfall (cumecs), catchment sediment loss through aeolian processes ( $\text{m}^3$ ), sediment discharged from the catchment through fluvial processes ( $\text{m}^3$ ) and the grainsize distribution of the sediment discharged by fluvial processes. The value of each of these variables is the cumulative over the defined output interval. The water balance created under the *Hydrology* tab will also create a daily time series, based on the water partitioning, surface water and groundwater components of the CLiDE platform.

### 4.4.2 Graphical

The *Generate Google Earth Animation* parameters (Figure 13) allow the graphics generated by the GUI to be directly exported to Google Earth using a .kmz file. Images will be automatically saved as .png files in a folder named *Animation* based in the CLiDE executable home folder. The time interval (mins) is specified in the appropriate box and the start date of the simulation must match those used for initialisation (Section 3.5). The graphical options selected in the GUI (Section 4.5) at the specified time interval will be captured in the resultant .png file.

### 4.4.3 Gridded

The temporal spacing of gridded output is controlled by the *Save files every (mins)* value (Figure 3). Every time the specified interval is reached a new set of gridded data is produced in the home folder from which the CLiDE executable was run. If the *Unique file name* option is selected, a time stamp is appended to every output gridded file. If this option is de-selected, each grid file is overwritten. The choice of which gridded data to save is made by selecting variables under the *Save Option* bar at the top of the GUI. Variables under this bar may be selected and deselected by clicking on the desired item. These save options will be recorded if an XML of the initialisation data is saved (Section 4.2)

#### 4.5 GRAPHICAL OPTIONS

The graphical output from the model may be toggled on and off using the *view tabs?* check box (Figure 13). The graphical properties may be controlled using the two slide bars close to the top of the GUI. The zoom bar allows increased magnification if dragged to the right and reduced magnification if dragged to the left. The contrast slide bar only effects some of the variables on display. It further increases the contrast between higher and lower values for visible datasets if dragged to the right. The selection of variables to display is undertaken using the *Top Graphics* and *Top Graphics II* bars at the top of the GUI. Variables may be selected or deselected using by clicking on that particular variable. Variables further down the list are overlain on variables that occur further up the list.

To save computation resources, graphics are only updated at the interval provided in the save gridded data option (Section 4.4.3) or by clicking the *update graphics* button.

## 5 Calibration

### 5.1 INTRODUCTION

Calibration (platform validation) is an important step in the modelling process where simulations are to represent, or make predictions for, a ‘real’ environment. Within the CLiDE platform there are currently three main processes that can be calibrated to observed data; the hydrology, fluvial sediment transport and debris flow. For each of these system components the calibration process relies on modifying the input or initialisation data to fit the simulated output to observed data.

### 5.2 HYDROLOGICAL

Calibrating the CLiDE platform hydrology consists of two distinct steps; the calibration of the surface runoff followed by the calibration of the groundwater module. Both of these steps may require a number of iterations before an acceptable match between observed and simulated data is found. Within the UK, gauged river data over a number of years is easily obtainable for major catchments.

#### 5.2.1 Surface Runoff

For this step in the calibration we are comparing the simulated surface runoff components to observed river gauging data. We therefore need to separate the runoff and baseflow components for both datasets before the comparison is made. This allows the separate influences on the different flow paths to be assessed and modified. The longer the calibration, the greater the certainty of the validation, both in terms of large scale climate trends and the response of the platform to short, intense events such as storms. Uncertainty may also be reduced by calibrating the platform to multiple, spatially distributed locations.

#### PREPARING THE GAUGED FLOW DATA

A baseflow separation is required for the gauged river flow dataset. There are several methods for the separation of baseflow from gauged river data (Eckhardt, 2008). The UKIH low flow method (Piggott et al., 2005) is one such technique that can be applied to daily data and is described in the following paragraph.

The UKIH method is based on periods of flow that are assumed to be composed entirely of baseflow, which occur within a time series of gauged river data. To identify these periods, the gauged data is divided into 5 day segments and the minimum values within each segment are selected. The low point for each segment,  $y_i$ , is compared to neighbouring (temporally) segments, and turning points along the sequence identified as low flows that satisfy the equation 5.1. The daily baseflow contribution to a river is estimated by linearly interpolating between these turning points.

$$0.9y_i < \min(y_{i-1}, y_{i+1}) \quad (5.1)$$

To create a baseflow separated time series of river flow, whereby only surface runoff contribution is included, the baseflow value at each point must be removed from the total gauged flow.

#### SIMULATION

Calibrating the simulated surface runoff requires the groundwater module to be disabled (Section 3.8), so that no baseflow is returned into river flows. For the calibration period, it is important that the platform has reached a quasi-steady (balanced) state, whereby soil moisture and surface water stores are no longer trying to reach equilibrium from their initialised state. This may be checked by monitoring the SMD and NSSS output from the water balance. Upon equilibrium both of these stores should show an annual cycle of variation, but no significant trend inter-annually.

Following confirmation of steady state, the platform is ready to undertake a calibration run. River flow at the location corresponding to that of the flow gauging station must be output during the simulation. With baseflow return disabled the simulated river flow is directly comparable to the baseflow separated river gauge data. If the two datasets do not match within acceptable limits, the initialisation and input parameters for the simulation must be re-assessed and the calibration repeated.

It is suggested that the following parameters are modified in order to attain a better match between simulated and gauged data:

#### *SLiM surface water partitioning (Hydrology tab)*

- Modifying the rooting depth imparts a change in water take up by the vegetation. Seasonal changes to this value represent annual changes in the growth cycle of vegetation. Increasing these values reduces the available water in the soil store and increases evapotranspiration rate. Again the response will not be related linearly to the change in forcing and is catchment specific.
- The rain interception coefficient represents a loss of rainfall (as a percentage) to unknown sinks.

#### *Lisflood surface water routing (Flow Model tab)*

- Parameters described in Section 3.9)



### 5.2.2 Groundwater

Once the surface water has been calibrated, the groundwater component may be calibrated to either; total gauged river flow (i.e., without the baseflow separation) or to groundwater head levels. The procedure for calibrating to total flow is similar to the surface water calibration. The key differences are, that the groundwater component is enabled during simulation and that the hydraulic conductivity and specific yield of the groundwater component are modified instead of the surface water components. If calibrating to groundwater head levels, the groundwater level output from the simulation must be saved for the required time period (Section 4.4.3). As with the surface water component, it is important the simulated system is in steady state for the calibration period. In the case of groundwater, this involves monitoring the groundwater head levels in the water balance to ensure they have reached an equilibrium condition that shows seasonal changes, but little inter-annual change.

When calibrating the groundwater module it is advised that only the multiplier values in the *Hydrology* tab are modified and not the distributed values. This avoids having to modify all of the values in the distributed groundwater input files after each iterative step of the calibration process.

- Increasing the hydraulic conductivity allows water to flow at a faster rate through the subsurface, creating a less steep gradient below high and low heads and reducing the time lag from recharge to baseflow return.
- The specific yield determines the groundwater head response to an incoming or outgoing flux of water. A groundwater system with a high specific yield will show a smaller response to the influx or removal of water in comparison to a catchment with a low specific yield.

### 5.3 DEBRIS FLOW

The debris flow component may be calibrated against observed data, using an iterative technique similar in principal to the hydrological calibration. There are two main parts to the calibration of debris flows; matching the physical characteristics of previous flows (for example, lateral runoff length and total flow area/volume), and matching the triggering of such events in time with respect to the driving hydrology. Both require the parameter values that drive the simulation to be updated, improving the match between model and observation after each iteration. The triggering characteristics of debris flow are controlled by the friction angle parameter under the slope processes tab (Section 3.12.3). The remaining SCIDDICA parameters determine the flow characteristics. D'Ambrosio et al. (2003) provide an extended description of the component calibration.

## 6 Troubleshooting

### OPENING EXECUTABLE

- Check the number of available screens on computer. If displaying on a projection, the model may be opening on a separate screen. This can be checked by searching the Applications list in Windows Task Manager for the CLiDE executable running.

### OPENING XML FILE

- If the XML file has been edited using a text editor, an item within the XML may have been renamed. Save a new XML under a different name and compare the name of each variable to the XML that is needed. Update differing variable names.
- An XML saved in an older version of CLiDE may not work with newer versions and vice versa due to a different list of variables required in the XML file. Save a new XML under a different name and compare the name of each variable to the XML that is needed. Update differing variable names.

### LOADING INITIALISATION DATA

- Check that the size of each array matches the other arrays and the header information.
- Check date information in *Setup* tab is as expected.
- Use a different text editor to view input files (line returns are picked up by some and not others). Notepad++ is recommended.

### SIMULATION FREEZES

- Allow the simulation time to process large amounts of data. When processing a catchment with a large number of nodes the daily timestep may take a few minutes to complete.
- Increase the amount of memory available to the program by reducing the memory limit in the *Setup* tab to 1.
- Check groundwater input file for zero, negative or small values (<10 m). If the groundwater reaches zero during the simulation this can cause instability. To prevent this, the entire catchment can be uplifted by adding 50 m to each nodal elevation in the DEM, bedrock and initial groundwater files. This can be removed during post-processing if required.
- Check rainfall and potential evapotranspiration data exist for the previous, current and proceeding timestep being simulated when the platform froze.
- Ensure output from previous simulation is not open in another program, as output files can not be over-written (as an exception, some text editors will allow this).

### NO OUTPUT IS PRODUCED

- Check the save file time in the *Setup* tab is as expected (a value of 1440 is daily).

- Check options are checked in the *Save Options* bar at the top of the GUI.
- Check you are in the CLiDE

## References

- Allen, R., Pereira, L.A., Raes, D., and Smith, M., 1998. Crop evapotranspiration: guidelines for computing crop water requirements. FAO, Irrigation and Drainage Paper No. 56. FAO, Rome, Italy.
- Bates, B.C., Kundzewicz, Z., Wu, S., and Palutikof, J., 2008. Climate Change and Water. Technical Paper of the Intergovernmental Panel on Climate Change, Geneva, 210 pp.
- Bates, P.D., Horritt, M.S., and Fewtrell, T.J., 2010. A simple inertial formulation of the shallow water equations for efficient two-dimensional flood inundation modelling. *J. Hydrol.*, 387, 33–45.
- Bevan, K.J., and Kirkby, M.J., 1979. A physically based, variable contributing area model of basin hydrology. *Hydrol. Sci. Bull.*, 24((1), 43-69.
- Boorman, D.B., Hollis, J.M., and Lilly, A., 1995. Hydrology of soil types: a hydrologically-based classification of the soils of the United Kingdom. Report No. 126, Institute of Hydrology, Wallingford, UK.
- Carson, M.A., and Kirkby, M.J., 1972. Hillslope Form and Process. Cambridge Geographical Studies No. 3., 475pp.
- Coulthard, T.J., 2001. Landscape evolution models: a software review. *Hydrol. Process.*, 15(1), 165-173.
- Coulthard, T.J., and Frostick, L.E., 2010. The Hull floods of 2007: implications for the governance and management of urban drainage systems. *J. Flood Risk Manage.*, 3(3), 1–9.
- Coulthard, T.J., and Van De Wiel, M.J., 2007. Quantifying fluvial non-linearity and finding self organized criticality? Insights from simulations of river basin evolution. *Geomorphology*, 91, 216-235.
- Coulthard, T.J., and Van de Wiel, M.J., 2006. A cellular model of river meandering. *Earth Surf. Proc. Land.*, 31, 123–132.
- Coulthard, T.J., Lewin, J., and Macklin, M.G., 2005. Modelling differential and complex catchment response to environmental change. *Geomorphology*, 69(1–4), 224–241.
- Coulthard, T. J., 2013. [https://code.google.com/p/caesar-lisflood/downloads/detail?name=grainfi\\_lemaker1.zip&can=2&q=](https://code.google.com/p/caesar-lisflood/downloads/detail?name=grainfi_lemaker1.zip&can=2&q=) (accessed 15th February 2014)
- Coulthard, T. J., Neal, J.C., Bates, P.D., Ramirez, J., de Almeida, G.A.M., and Hancock, G. R., 2013. Integrating the LISFLOOD-FP 2D hydrodynamic model with the CAESAR model: implications for modelling landscape evolution. *Earth Surf. Process. Land.*, 38, 1897–1906.
- D'Ambrosio, D., Di Gregorio, S., and Iovine, G., 2003 Simulating debris flows through a hexagonal cellular automata model: SCIDDICA S3–hex. *Nat. Haz. Earth Syst. Sci.*, 3, 545–559.
- Di Gregorio, S., Rongo, R., Siciliano, C., Sorriso-Valvo, M., and Spataro, W.: Mount Ontake landslide simulation by the cellular automata model SCIDDICA-3, *Physics and Chemistry of the Earth*, 24, 97–100, 1999.
- Dietrich, W.E., Bellugi, D., Heimsath, A.M., Roering, J.J., Sklar, L. & Stock, J.D. 2003. Geomorphic transport laws for predicting the form and evolution of landscapes. In P. Wilcock & R. Iverson (eds.), *Prediction in Geomorphology*. American Geophysical Union Monograph Series 135: 103-132.
- Eckhardt, K., 2008. A comparison of baseflow indices, which were calculated with seven different baseflow separation methods. *J. Hydrol.*, 352, 168–173.

- Einstein, H.A., 1950. The bed-load function for sediment transportation in open channel flows. Technical Bulletin 1026, USDA, Soil Conservation Science, 1–77.
- Haitjema, H.M., 1995. Analytic Element Modeling of Groundwater Flow, Academic Press, 394pp.
- Hancock, G.R., Coulthard, T.J., Martinez, C., and Kalma, J.D., 2011. An evaluation of landscape evolution models to simulate decadal and centennial scale soil erosion in grassland catchments. *J. Hydrol.*, 308, 171–183.
- Hoffmann, T., Thorndycraft, V.R., Brown, A.G., Coulthard, T.J., Damnati, B., Kale, V.S., Middelkoop, H., Notebaert, B., and Walling, D., 2010. Human impact on fluvial regimes and sediment flux during the Holocene: Review and future research agenda. *Global Planet. Change*, 72(3), 87–98.
- Hough M.N. and Jones, R.J.A., 1997. The United Kingdom Meteorological Office rainfall and evaporation calculation system: MORECS version 2.0 — an overview. *Hydrol. Earth Sys. Sci.*, 1, 227–239.
- Kinnell, P.I.A., 2010. Event soil loss, runoff and the Universal Soil Loss Equation family of models: A review. *J. Hydrol.*, 385(1–4), 384–397.
- Korup O., Montgomery D.R., and Hewitt K., 2010. Glacier and landslide feedbacks to topographic relief in the Himalayan syntaxes. *Proc Natl Acad Sci U S A*. 2010 Mar 23, 107(12), 5317–22.
- Liang, D., Falconer, R.A., and Lin, B., 2006. Improved numerical modelling of estuarine flows. *Proceedings of the Institution of Civil Engineers, Maritime Engineering*, 159 (1), 25–35
- Metha, A., and Barker, G.C., 1994. The dynamics of sand. *Rep. Prog. Phys.*, 57(4), 385–416.
- Morton, D., Rowland, C., Wood, C., Meek, L., Marston, C., Smith, G., Wadsworth, R., Simpson, I.C., 2011. Final Report for LCM2007 – the new UK Land Cover Map. Centre for Ecology and Hydrology, Lancaster, 115pp.
- Murray, A.B., and Paola, C., 1994. A cellular model of braided rivers. *Nature*, 371, 54–57.
- Murray, A.B., and Paola, C., 1997. Properties of a cellular braided-stream model. *Earth Surf. Proc. Land.*, 22, 1001–1025.
- Murray, A.B., and Paola, C., 2003. Modelling the effect of vegetation on channel pattern in bedload rivers. *Earth Surf. Proc. Land.*, 28, 131–143.
- Pack, R.T., Tarboton, D.G., and Goodwin, C.N., 2001. Assessing terrain stability in a GIS using SINMAP, in 15th annual GIS conference, Vancouver, British Columbia, 19–22 February 2001.
- Piggott, A.R., Moin, S., and Southam, C., 2009. A revised approach to the UKIH method for the calculation of baseflow. *Hydrological Sciences Journal*, 50(5), 911–920.
- Ravazzani, G., Rametta, D., and Mancini, M., 2011. Macroscopic cellular automata for groundwater modelling: A first approach. *Environ. Modell. Softw.*, 26 (5), 634–643.
- Reneau, S.L., and Dietrich, W.E., 1987. Size and location of colluvial landslides in a steep forested landscape, Proceedings of the International Symposium on Erosion and Sedimentation in the Pacific Rim. Corvallis, Oregon., August 3-7, 1987. *IAHS Bulletin* 165: 39–48.
- Roache, P.J., 1976. *Computational Fluid Dynamics*. Albuquerque, NM: Hermosa. Rev. 1976.
- Rosso, R., Rulli, M.C., and Vannucchi, G., 2006. A physically based model for hydrologic control on shallow landsliding. *Water Resources Research* 42: W06410.

- Rothman, D.H., 1988. Cellular-automaton fluids: A model for flow in porous media. *Geophys.*, 53(4), 509–518.
- Rushton, K.R., 2003. *Groundwater hydrology: conceptual and computational models*. John Wiley and Sons Ltd, West Sussex, England.
- Selby, M.J., 1993. *Hillslope Materials and Processes*. Oxford Univ. Press, Oxford, UK, 451 pp.
- Tooth, S., Jansen, J.D., Nanson, G., Coulthard, T.J., and Pietsch, T., 2008. Riparian vegetation and the late Holocene development of an anabranching river: Magela Creek, northern Australia. *GSA Bull.*, 120(7-8), 1021–1035.
- Tucker, G.E., and Hancock, G.R., 2010. Modelling landscape evolution. *Earth Surf. Proc. Land.*, 35(1), 28–50.
- Van de Wiel, M.J., Coulthard, T.J., Macklin, M.G., and Lewin, J., 2011. Modelling the response of river systems to environmental change: Progress, problems and prospects for palaeo-environmental reconstructions. *Earth Sci. Rev.*, 104(1-3), 167–185.
- Van der Knijff, J.M., Younis, J., and De Roo, A.P.J., 2010. LISFLOOD: a GIS-based distributed model for river basin scale water balance and flood simulation. *Int. J. Geogr. Inf. Sci.*, 24, 189-212.
- Wang, J.F., and Anderson, M.P., 1982. *Introduction to Groundwater Modelling*. Freeman, San Francisco, CA, USA.
- Wang, L., Barkwith, A., Jackson, C., and Ellis, M., 2012. SLiM : an improved soil moisture balance method to simulate runoff and potential groundwater recharge processes using spatio-temporal weather and catchment characteristics. 12th UK CARE Annual General Meeting, UK Chinese Association of Resources and Environment, Bristol, UK, 8 Sept 2012.
- Wilcock, P., and Crowe, J., 2003. Surface-based transport modelling for mixed-size sediment. *J. Hydraul. Eng.*, 129(2), 120–128.